



A space–time DG method for the Schrödinger equation with variable potential

Sergio Gómez¹ · Andrea Moiola²

Received: 21 June 2023 / Accepted: 16 January 2024 / Published online: 1 March 2024
© The Author(s) 2024

Abstract

We present a space–time ultra-weak discontinuous Galerkin discretization of the linear Schrödinger equation with variable potential. The proposed method is well-posed and quasi-optimal in mesh-dependent norms for very general discrete spaces. Optimal h -convergence error estimates are derived for the method when test and trial spaces are chosen either as piecewise polynomials or as a novel quasi-Trefftz polynomial space. The latter allows for a substantial reduction of the number of degrees of freedom and admits piecewise-smooth potentials. Several numerical experiments validate the accuracy and advantages of the proposed method.

Keywords Schrödinger equation · Ultra-weak formulation · Discontinuous Galerkin method · Smooth potential · Quasi-Trefftz space

Mathematics Subject Classification (2010) 65M60 · 78M10 · 35Q41

1 Introduction

In this work we are interested in the approximation of the solution to the time-dependent Schrödinger equation on a space–time cylinder $Q_T = \Omega \times I$, where $\Omega \subset \mathbb{R}^d$ ($d \in \mathbb{N}$) is an open, bounded polytopic domain with Lipschitz boundary $\partial\Omega$, and $I = (0, T)$ for some final time $T > 0$:

$$S\psi := i\partial_t\psi + \frac{1}{2}\Delta_{\mathbf{x}}\psi - V\psi = 0 \quad \text{in } Q_T,$$

✉ Sergio Gómez
sergio.gomezmacias@unimib.it

Andrea Moiola
andrea.moiola@unipv.it

¹ Department of Mathematics and Applications, University of Milano-Bicocca, Via Cozzi 55, 20125 Milan, Italy

² Department of Mathematics, University of Pavia, Via Ferrata 5, 27100 Pavia, Italy

$$\begin{aligned}
\psi &= g_D && \text{on } \Gamma_D \times I, \\
\partial_{\mathbf{n}_x} \psi &= g_N && \text{on } \Gamma_N \times I, \\
\partial_{\mathbf{n}_x} \psi - i \vartheta \psi &= g_R && \text{on } \Gamma_R \times I, \\
\psi(\mathbf{x}, 0) &= \psi_0(\mathbf{x}) && \text{on } \Omega.
\end{aligned} \tag{1.1}$$

Here i is the imaginary unit; $\partial_{\mathbf{n}_x}(\cdot)$ is the normal derivative-in-space operator; $V : Q_T \rightarrow \mathbb{R}$ is the potential energy function; $\vartheta \in L^\infty(\Gamma_R \times I)$ is a positive “impedance” function; the Dirichlet (g_D), Neumann (g_N), Robin (g_R) and initial condition (ψ_0) data are given functions; $\Gamma_D, \Gamma_N, \Gamma_R$ are a polytopic partition of $\partial\Omega$.

The model problem (1.1) has a wide range of applications. In quantum physics [25], the solution ψ is a quantum-mechanical wave function determining the dynamics of one or multiple particles in a potential V . In electromagnetic wave propagation [24], it is called “paraxial wave equation” and ψ is a function associated with the field component in a two-dimensional electromagnetic problem where the energy propagates at small angles from a preferred direction. In such problems, the function V depends on the refractive index and the wave number. In underwater sound propagation [22], it is referred to as “parabolic equation” and ψ describes a time-harmonic wave propagating primarily in one direction. In molecular dynamics [2], by neglecting the motion of the atomic nuclei, the Born-Oppenheimer approximation leads to a Schrödinger equation in the *semi-classical* regime.

Space–time Galerkin methods discretize all the variables in a time-dependent PDE at once; this is in contrast with the method of lines, which combines a spatial discretization and a time-stepping scheme. Space–time methods can achieve high convergence rates in space and time, and provide discrete solutions that are available on the whole space–time domain.

The literature on space–time Galerkin methods for the Schrödinger equation is very scarce. In fact, the standard Petrov-Galerkin formulation for the Schrödinger equation, i.e., the analogous formulation to that proposed in [32] for the heat equation, is not inf-sup stable, see [14, Sect. 2.2]. In [20], Karakashian and Makridakis proposed a space–time method for the Schrödinger equation with nonlinear potential, combining a conforming Galerkin discretization in space and an upwind DG time-stepping. This method reduces to a Radau IIA Runge–Kutta time discretization in the case of constant potentials. Moreover, under some restrictions on the mesh that are necessary to preserve the accuracy of the method, it allows for changing the spatial mesh on each time-slab, but not for local time-stepping. A second version of the method, obtained by enforcing the transmission of information from the past through a projection, was proposed in [21]. This version reduces to a Legendre Runge–Kutta time discretization in the case of constant potentials. Recently, some space–time methods based on ultra-weak formulations of the Schrödinger equation have been designed. The well-posedness of such formulations requires weaker assumptions on the mesh. Demkowicz et al., in [8], the authors proposed a discontinuous Petrov-Galerkin (DPG) formulation for the linear Schrödinger equation. The method is a conforming discretization of an ultra-weak formulation of the Schrödinger equation in graph spaces. Well-posedness and quasi-optimality of the method follow directly from the inf-sup stability (in a

graph norm) of the continuous Petrov–Galerkin formulation. In [14], Hain and Urban proposed a space–time ultra-weak variational formulation for the Schrödinger equation with optimal inf-sup constant. The formulation in [14] is closely related to the DPG method in [8], but differs in the choice of the test and trial spaces. While for the method in [8] one first fixes a trial space and then construct a suitable test space, the method in [14] requires the choice of a conforming test space and then the trial space is defined accordingly. We are not aware of publications proposing space–time DG methods for the Schrödinger equation other than [8, 14, 20, 21], outlined in this paragraph, and the space–time Trefftz DG method in [11, 12], which motivated the present paper.

Trefftz methods are Galerkin discretizations with test and trial spaces spanned by local solutions of the considered PDE. Trefftz methods with lower-dimensional spaces than standard finite element spaces, but similar approximation properties, have been designed for many problems, e.g., Laplace and solid-mechanics problems [31]; the Helmholtz equation [16]; the time-harmonic [15], and time-dependent [10] Maxwell’s equations; the acoustic wave equation in second-order [1] and first-order [27] form; the Schrödinger equation [11]; among others. Nonetheless, pure Trefftz methods are essentially limited to problems with piecewise-constant coefficients, as for PDEs with varying coefficients the design of “rich enough” finite-dimensional Trefftz spaces is in general not possible. A way to overcome this limitation is the use of quasi-Trefftz methods, which are based on spaces containing functions that are just approximate local solutions to the PDE. In essence, the earliest quasi-Trefftz spaces are the generalized plane waves used in [17] for the discretization of the Helmholtz equation with smoothly varying coefficients. More recently, a quasi-Trefftz DG method for the acoustic wave equation with piecewise-smooth material parameters was proposed in [19], where some polynomial quasi-Trefftz spaces were introduced. As an alternative idea, the embedded Trefftz DG method proposed in [23] does not require the local basis functions to be known in advance, as they are simply taken as a basis for the kernel of the local discrete operators in a standard DG formulation. This corresponds to a Galerkin projection of a DG formulation with a predetermined discrete space onto a Trefftz-type subspace. In practice, it requires the computation of singular or eigenvalue decompositions of the local matrices.

In [11], the authors proposed a space–time Trefftz DG method for the Schrödinger equation with piecewise-constant potential, whose well-posedness and quasi-optimality in mesh-dependent norms were proven for general discrete Trefftz spaces. Optimal h -convergence estimates were shown in [11] for a Trefftz space consisting of complex exponential wave functions, and in [12] for a polynomial Trefftz space.

In this work we propose a space–time DG method for the discretization of the Schrödinger equation with variable potentials, extending the formulation of [11] to more general problems and discrete spaces. The main advantages of the proposed method are the following:

- The proposed ultra-weak DG variational formulation of (1.1) is well-posed, stable, and quasi-optimal in any space dimension for an almost arbitrary choice of piecewise-defined discrete spaces and variable potentials.

- A priori error estimates in a mesh-dependent norm can be obtained by simply analyzing the approximation properties of the local spaces.
- The method naturally allows for non-matching space-like and time-like facets and all our theoretical results hold under standard assumptions on the space–time mesh, which make the method suitable for adaptive versions and local time-stepping.
- Building on [19], for elementwise smooth potentials, we design and analyze a quasi-Trefftz polynomial space with similar approximation properties of full polynomial spaces but with much smaller dimension, thus substantially reducing the total number of degrees of freedom required for a given accuracy.

Structure of the paper In Sect. 2 we introduce some notation on the space–time meshes to be used and the proposed ultra-weak DG variational formulation on abstract spaces. Section 3 is devoted to the analysis of well-posedness, stability and quasi-optimality of the method. In Sects. 4.2 and 4.3 we prove optimal h -convergence estimates for the method when the test and trial spaces are taken as the space of piecewise polynomials or a novel quasi-Trefftz space, respectively. In Sect. 5 we present some numerical experiments that validate our theoretical results and illustrate the advantages of the proposed method. We end with some concluding remarks in Sect. 6.

2 Ultra-weak discontinuous Galerkin formulation

2.1 Space–time mesh and DG notation

Let \mathcal{T}_h be a non-overlapping prismatic partition of Q_T , i.e., each element $K \in \mathcal{T}_h$ can be written as $K = K_x \times K_t$ for a d -dimensional polytope $K_x \subset \Omega$ and a time interval $K_t \subset I$. We use the notation $h_{K_x} = \text{diam}(K_x)$, $h_{K_t} = |K_t|$ and $h_K = \text{diam}(K) = (h_{K_x}^2 + h_{K_t}^2)^{1/2}$. We call “mesh facet” any intersection $F = \partial K_1 \cap \partial K_2$ or $F = \partial K_1 \cap \partial Q_T$, for $K_1, K_2 \in \mathcal{T}_h$, that has positive d -dimensional measure and is contained in a d -dimensional hyperplane. We denote by $\bar{\mathbf{n}}_F = (\bar{\mathbf{n}}_F^x, n_F^t) \in \mathbb{R}^{d+1}$ one of the two unit normal vectors orthogonal to F with $n_F^t = 0$ or $n_F^t = 1$. We assume that each internal mesh facet F is either

a space-like facet if $\bar{\mathbf{n}}_F^x = 0$, or a time-like facet if $n_F^t = 0$.

We further denote the mesh skeleton and its parts as

$$\begin{aligned}\mathcal{F}_h &:= \bigcup_{K \in \mathcal{T}_h} \partial K, & \mathcal{F}_h^0 &:= \Omega \times \{0\}, & \mathcal{F}_h^T &:= \Omega \times \{T\}, \\ \mathcal{F}_h^D &:= \Gamma_D \times (0, T), & \mathcal{F}_h^N &:= \Gamma_N \times (0, T), & \mathcal{F}_h^R &:= \Gamma_R \times (0, T), \\ \mathcal{F}_h^{\text{time}} &:= \text{the union of all the internal time-like facets}, \\ \mathcal{F}_h^{\text{space}} &:= \text{the union of all the internal space-like facets}.\end{aligned}$$

We employ the standard DG notation for the averages $\{\cdot\}$ and space $\llbracket \cdot \rrbracket_{\mathbf{N}}$ and time $\llbracket \cdot \rrbracket_t$ jumps for piecewise complex scalar w and vector $\boldsymbol{\tau}$ fields:

$$\begin{aligned} \begin{cases} \{w\} := \frac{1}{2} (w|_{K_1} + w|_{K_2}) \\ \{\boldsymbol{\tau}\} := \frac{1}{2} (\boldsymbol{\tau}|_{K_1} + \boldsymbol{\tau}|_{K_2}) \end{cases} & \quad \text{on } \partial K_1 \cap \partial K_2 \subset \mathcal{F}_h^{\text{time}}, \\ \begin{cases} \llbracket w \rrbracket_{\mathbf{N}} := w|_{K_1} \bar{\mathbf{n}}_{K_1}^{\mathbf{x}} + w|_{K_2} \bar{\mathbf{n}}_{K_2}^{\mathbf{x}} \\ \llbracket \boldsymbol{\tau} \rrbracket_{\mathbf{N}} := \boldsymbol{\tau}|_{K_1} \cdot \bar{\mathbf{n}}_{K_1}^{\mathbf{x}} + \boldsymbol{\tau}|_{K_2} \cdot \bar{\mathbf{n}}_{K_2}^{\mathbf{x}} \end{cases} & \quad \text{on } \partial K_1 \cap \partial K_2 \subset \mathcal{F}_h^{\text{time}}, \\ \llbracket w \rrbracket_t := w|_{K_1} n_{K_1}^t + w|_{K_2} n_{K_2}^t = w^- - w^+, & \quad \text{on } \partial K_1 \cap \partial K_2 \subset \mathcal{F}_h^{\text{space}}, \end{aligned}$$

where $\bar{\mathbf{n}}_K^{\mathbf{x}} \in \mathbb{R}^d$ and $n_K^t \in \mathbb{R}$ are the space and time components of the outward-pointing unit normal vectors on $\partial K \cap \mathcal{F}_h^{\text{time}}$ and $\partial K \cap \mathcal{F}_h^{\text{space}}$, respectively. The superscripts “−” and “+” are used to denote the traces of a function on a space-like facet from the elements “before” (−) and “after” (+) the facet.

The space–time prismatic meshes described in this section may include hanging space-like and time-like facets, so the proposed method allows for local time-stepping and local space–time refinements. Tent-pitched meshes are popular in space–time methods for wave propagation problems; see, e.g., [30] and [27, Eq. 3]. However, such meshes approximate the solution to the Schrödinger equation do not lead to a semi-implicit discretization of the Schrödinger equation because the propagation speed of its solutions, which dictates the slope of space-like facets of the tents, is infinite.

We denote space–time broken function spaces as $H^s(\mathcal{T}_h) := \{v \in L^2(Q_T), v|_K \in H^s(K) \forall K \in \mathcal{T}_h\}$, $\mathcal{C}^s(\mathcal{T}_h) := \{v : Q_T \rightarrow \mathbb{C}, v|_K \in \mathcal{C}^s(K) \forall K \in \mathcal{T}_h\}$, for $s \in \mathbb{N}_0$.

2.2 Variational formulation of the DG method

For any finite-dimensional subspace $\mathbb{V}_{hp}(\mathcal{T}_h)$ of the broken Bochner–Sobolev space

$$\mathbf{V}(\mathcal{T}_h) := \prod_{K \in \mathcal{T}_h} H^1(K_t; L^2(K_{\mathbf{x}})) \cap L^2(K_t; H^2(K_{\mathbf{x}})),$$

the proposed ultra-weak DG variational formulation for the Schrödinger equation (1.1) is:

$$\text{Seek } \psi_{hp} \in \mathbb{V}_{hp}(\mathcal{T}_h) \text{ such that: } \mathcal{A}(\psi_{hp}; v_{hp}) = \ell(v_{hp}) \quad \forall v_{hp} \in \mathbb{V}_{hp}(\mathcal{T}_h), \quad (2.1)$$

where

$$\begin{aligned} \mathcal{A}(\psi_{hp}; v_{hp}) := & \sum_{K \in \mathcal{T}_h} \int_K \psi_{hp} \overline{\mathcal{S}v_{hp}} \, dV + i \left(\int_{\mathcal{F}_h^{\text{space}}} \psi_{hp}^- \llbracket \overline{v_{hp}} \rrbracket_t \, d\mathbf{x} + \int_{\mathcal{F}_h^t} \psi_{hp} \overline{v_{hp}} \, d\mathbf{x} \right) \\ & + \frac{1}{2} \int_{\mathcal{F}_h^{\text{time}}} \left(\llbracket \nabla_{\mathbf{x}} \psi_{hp} \rrbracket \cdot \llbracket \overline{v_{hp}} \rrbracket_{\mathbf{N}} + i\alpha \llbracket \psi_{hp} \rrbracket_{\mathbf{N}} \cdot \llbracket \overline{v_{hp}} \rrbracket_{\mathbf{N}} \right) \end{aligned}$$

$$\begin{aligned}
& - \left\{ \psi_{hp} \right\} \left[\nabla_{\mathbf{x}} \overline{v_{hp}} \right]_{\mathbf{N}} + i \beta \left[\nabla_{\mathbf{x}} \psi_{hp} \right]_{\mathbf{N}} \left[\nabla_{\mathbf{x}} \overline{v_{hp}} \right]_{\mathbf{N}} \right) dS \\
& + \frac{1}{2} \int_{\mathcal{F}_h^{\mathcal{D}}} (\partial_{\mathbf{n}_{\mathbf{x}}} \psi_{hp} + i \alpha \psi_{hp}) \overline{v_{hp}} dS \\
& + \frac{1}{2} \int_{\mathcal{F}_h^{\mathcal{N}}} (-\psi_{hp} \partial_{\mathbf{n}_{\mathbf{x}}} \overline{v_{hp}} + i \beta (\partial_{\mathbf{n}_{\mathbf{x}}} \psi_{hp}) (\partial_{\mathbf{n}_{\mathbf{x}}} \overline{v_{hp}})) dS \\
& + \frac{1}{2} \int_{\mathcal{F}_h^{\mathcal{R}}} (\delta \partial_{\mathbf{n}_{\mathbf{x}}} \psi_{hp} + (1 - \delta) i \vartheta \psi_{hp}) \left(\overline{v_{hp}} + \frac{i}{\vartheta} \partial_{\mathbf{n}_{\mathbf{x}}} \overline{v_{hp}} \right) dS \\
& + i \sum_{K \in \mathcal{T}_h} \int_K \mu \mathcal{S} \psi_{hp} \overline{\mathcal{S} v_{hp}} dV, \\
\ell(v_{hp}) := & i \int_{\mathcal{F}_h^{\mathcal{D}}} \psi_0 \overline{v_{hp}} d\mathbf{x} + \frac{1}{2} \int_{\mathcal{F}_h^{\mathcal{D}}} g_{\mathcal{D}} (\partial_{\mathbf{n}_{\mathbf{x}}} \overline{v_{hp}} + i \alpha \overline{v_{hp}}) dS \\
& + \frac{1}{2} \int_{\mathcal{F}_h^{\mathcal{N}}} g_{\mathcal{N}} (-\overline{v_{hp}} + i \beta \partial_{\mathbf{n}_{\mathbf{x}}} \overline{v_{hp}}) dS \\
& + \frac{1}{2} \int_{\mathcal{F}_h^{\mathcal{R}}} g_{\mathcal{R}} \left((\delta - 1) \overline{v_{hp}} + \frac{i \delta}{\vartheta} \partial_{\mathbf{n}_{\mathbf{x}}} \overline{v_{hp}} \right) dS,
\end{aligned}$$

for some mesh-dependent stabilization functions

$$\begin{aligned}
\alpha & \in L^\infty(\mathcal{F}_h^{\text{time}} \cup \mathcal{F}_h^{\mathcal{D}}), & \text{ess inf}_{\mathcal{F}_h^{\text{time}} \cup \mathcal{F}_h^{\mathcal{D}}} \alpha &> 0, \\
\beta & \in L^\infty(\mathcal{F}_h^{\text{time}} \cup \mathcal{F}_h^{\mathcal{N}}), & \text{ess inf}_{\mathcal{F}_h^{\text{time}} \cup \mathcal{F}_h^{\mathcal{N}}} \beta &> 0, \\
\delta & \in L^\infty(\mathcal{F}_h^{\mathcal{R}}), & 0 < \delta &\leq \frac{1}{2}, \\
\mu & \in L^\infty(Q_T), & \text{ess inf}_{Q_T} \mu &> 0.
\end{aligned}$$

More conditions on these functions, in particular on their dependence on the local mesh size, will be specified in Sect. 4.

The variational formulation (2.1) can be derived by integrating by parts twice in space and once in time in each element as in [11], and treating the Neumann and the Robin boundary terms similarly to [11, Rem. 3.7]. However, as the current setting does not require the discrete space $\mathbb{V}_{hp}(\mathcal{T}_h)$ to satisfy the Trefftz property ($\mathcal{S}\psi|_K = 0$, $\forall K \in \mathcal{T}_h$), there are an additional volume term that is needed to ensure consistency (the first integral over K in $\mathcal{A}(\cdot; \cdot)$), and a local *Galerkin-least squares* correction term (the second integral over K in $\mathcal{A}(\cdot; \cdot)$) that were not present in the previous method. Such additional terms vanish when $\mathbb{V}_{hp}(\mathcal{T}_h)$ is a discrete Trefftz space, thus recovering the formulation in [11].

Remark 1 (Implicit time-stepping through time-slabs). *The variational problem (2.1) is a global problem involving all the degrees of freedom of the discrete solution for the whole space-time cylinder Q_T . However, as upwind numerical fluxes are taken on the space-like facets, if the space-time prismatic mesh \mathcal{T}_h can be decomposed into time-slabs (i.e., if the mesh elements can be grouped in sets of the form $\Omega \times [t_{n-1}, t_n]$*

for a partition of the time interval of the form $0 = t_0 < t_1 < \dots < t_N = T$), the global linear system stemming from (2.1) can be solved as a sequence of N smaller systems of the form

$$\mathbf{K}_n \Psi_h^{(n)} = b_n \quad 1 \leq n \leq N,$$

where $b_n = \mathbf{R}_n \Psi_h^{(n-1)}$ for $n = 2, \dots, N$. This is comparable to an implicit time-stepping, and it naturally allows for local mesh refinement in different regions of the space–time cylinder Q_T . Moreover, when \mathcal{T}_h is a tensor-product space–time mesh, the potential V does not vary in time, and the partition of the time interval is uniform, the matrices \mathbf{K}_n and \mathbf{R}_n are the same for every time-slab.

Remark 2 (Self-adjointness and volume penalty term). The well-posedness of the variational formulation (2.1) strongly relies on the $L^2(K)$ -self-adjointness of the Schrödinger operator $\mathcal{S}(\cdot)$ on each $K \in \mathcal{T}_h$ (in the sense that $\int_K \mathcal{S}\psi \bar{\varphi} \, dV = \int_K \psi \overline{\mathcal{S}\varphi} \, dV$ for all $\psi \in \mathbf{V}(\mathcal{T}_h)$, $\varphi \in C_0^\infty(K)$), thanks to the fact that the only odd derivative in \mathcal{S} is multiplied to the imaginary unit), which makes the local Galerkin-least squares correction term consistent. On the one hand, such term is essential in the proof of coercivity of the sesquilinear form $\mathcal{A}(\cdot; \cdot)$ (see Proposition 1 below). On the other hand, numerical experiments suggest that it can be neglected without losing accuracy and stability, see Sect. 5.1.2 below. This is also the case for the quasi-Trefftz DG method for the Helmholtz equation [18, §5.1.3] and for the wave equation [19, §5.1], where a similar correction term was used. Nonetheless, in the design of an ultra-weak DG discretization for a PDE with a non-self-adjoint differential operator $\mathcal{L}(\cdot)$ (e.g., the heat operator $\mathcal{L}(\cdot) = (\partial_t - \Delta_{\mathbf{x}})(\cdot)$), the corresponding local least squares correction term $\sum_{K \in \mathcal{T}_h} \int_K \mu \mathcal{L}\psi_{hp} \overline{\mathcal{L}v_{hp}} \, dV$ would not control the consistency term $\sum_{K \in \mathcal{T}_h} \int_K \psi_{hp} \overline{\mathcal{L}^* v_{hp}} \, dV$ arising from the integration by parts.

Remark 3 (Time-dependent potentials). The variational problem (2.1) allows for time-dependent potentials V . This is an important feature as, in such a case, the method of separation of variables cannot be used to reduce the time-dependent problem (1.1) to the time-independent Schrödinger equation.

3 Well-posedness, stability and quasi-optimality of the DG method

The theoretical results in this section are derived for any spatial dimension d , and are independent of the specific choice of the discrete space $\mathbb{V}_{hp}(\mathcal{T}_h)$.

Recalling that the volume penalty function μ , the stabilization functions α , β and the impedance function ϑ are positive, and that $\delta \in (0, \frac{1}{2})$, we define the following mesh-dependent norms on $\mathbf{V}(\mathcal{T}_h)$:¹

$$|||w|||_{\text{DG}}^2 := \sum_{K \in \mathcal{T}_h} \left\| \mu^{\frac{1}{2}} \mathcal{S}w \right\|_{L^2(K)}^2 + \frac{1}{2} \left(\| \llbracket w \rrbracket_t \|_{L^2(\mathcal{F}_h^{\text{space}})}^2 + \| w \|_{L^2(\mathcal{F}_h^T \cup \mathcal{F}_h^0)}^2 \right)$$

¹ Observe that a factor $\frac{1}{2}$ is missing in the first term of the DG norm in [11, Eqn. (3.2)].

$$\begin{aligned}
& + \frac{1}{2} \left(\left\| \alpha^{\frac{1}{2}} \llbracket w \rrbracket_{\mathbf{N}} \right\|_{L^2(\mathcal{F}_h^{\text{time}})^d}^2 + \left\| \beta^{\frac{1}{2}} \llbracket \nabla_{\mathbf{x}} w \rrbracket_{\mathbf{N}} \right\|_{L^2(\mathcal{F}_h^{\text{time}})}^2 + \left\| \alpha^{\frac{1}{2}} w \right\|_{L^2(\mathcal{F}_h^{\text{D}})}^2 \right. \\
& \left. + \left\| \beta^{\frac{1}{2}} \partial_{\mathbf{n}_{\mathbf{x}}} w \right\|_{L^2(\mathcal{F}_h^{\text{N}})}^2 + \left\| (\vartheta(1-\delta))^{\frac{1}{2}} w \right\|_{L^2(\mathcal{F}_h^{\text{R}})}^2 + \left\| (\delta\vartheta^{-1})^{\frac{1}{2}} \partial_{\mathbf{n}_{\mathbf{x}}} w \right\|_{L^2(\mathcal{F}_h^{\text{R}})}^2 \right), \\
|||w|||_{\text{DG}^+}^2 &:= |||w|||_{\text{DG}}^2 + \sum_{K \in \mathcal{T}_h} \left\| \mu^{-\frac{1}{2}} w \right\|_{L^2(K)}^2 + \frac{1}{2} \left\| w^- \right\|_{L^2(\mathcal{F}_h^{\text{space}})}^2 \\
& + \frac{1}{2} \left(\left\| \alpha^{-\frac{1}{2}} \{ \nabla_{\mathbf{x}} w \} \right\|_{L^2(\mathcal{F}_h^{\text{time}})^d}^2 + \left\| \alpha^{-\frac{1}{2}} \partial_{\mathbf{n}_{\mathbf{x}}} w \right\|_{L^2(\mathcal{F}_h^{\text{D}})}^2 \right. \\
& \left. + \left\| \beta^{-\frac{1}{2}} \{ w \} \right\|_{L^2(\mathcal{F}_h^{\text{time}})}^2 + \left\| \beta^{-\frac{1}{2}} w \right\|_{L^2(\mathcal{F}_h^{\text{N}})}^2 + \left\| \delta^{-\frac{1}{2}} \vartheta^{\frac{1}{2}} w \right\|_{L^2(\mathcal{F}_h^{\text{R}})}^2 \right). \tag{3.2}
\end{aligned}$$

The sum of the $L^2(K)$ -type terms ensures that $||| \cdot |||_{\text{DG}^+}$ is a norm. That $||| \cdot |||_{\text{DG}}$ is a norm on $\mathbf{V}(\mathcal{T}_h)$ follows from the following reasoning (see also [11, Lemma 3.1]): if $w \in \mathbf{V}(\mathcal{T}_h)$ and $\|w\|_{\text{DG}} = 0$, then w is the unique variational solution to the Schrödinger equation (1.1) with homogeneous initial and boundary conditions. Moreover, by the energy conservation (if $\mathcal{F}_h^{\text{R}} = \emptyset$) or dissipation (if $\mathcal{F}_h^{\text{R}} \neq \emptyset$), then $\|w(\cdot, t)\|_{L^2(\Omega)}^2 \leq \|w(\cdot, 0)\|_{L^2(\Omega)}^2 = 0$, for all $t \in (0, T]$; therefore, $w = 0$.

The DG norms in (3.1)–(3.2) are chosen in order to ensure the following properties of the sesquilinear form $\mathcal{A}(\cdot; \cdot)$ and the antilinear functional $\ell(\cdot)$, from which the well-posedness and quasi-optimality of the method (2.1) follow.

Proposition 1 (Coercivity). *For all $w \in \mathbf{V}(\mathcal{T}_h)$ the following identity holds*

$$\Im(\mathcal{A}(w; w)) = |||w|||_{\text{DG}}^2.$$

Proof The result follows from the following identities (see [11, Prop. 3.2] for more details):

$$\begin{aligned}
\int_{\mathcal{F}_h^{\text{space}}} \left(\Re(v^- \llbracket \bar{v} \rrbracket_t) - \frac{1}{2} \llbracket |v|^2 \rrbracket_t \right) d\mathbf{x} &= \frac{1}{2} \int_{\mathcal{F}_h^{\text{space}}} |\llbracket v \rrbracket_t|^2 d\mathbf{x} \quad \forall v \in H^1(\mathcal{T}_h), \\
\int_{\mathcal{F}_h^{\text{time}}} (\{v\} \llbracket \tau \rrbracket_{\mathbf{N}} + \{\tau\} \cdot \llbracket v \rrbracket_{\mathbf{N}}) dS &= \int_{\mathcal{F}_h^{\text{time}}} \llbracket v \tau \rrbracket_{\mathbf{N}} dS \quad \forall (v, \tau) \in H^1(\mathcal{T}_h) \times H^1(\mathcal{T}_h)^d, \\
\Im \left(\sum_{K \in \mathcal{T}_h} \int_K w \overline{S w} dV \right) &= -\frac{1}{2} \left(\int_{\mathcal{F}_h^{\text{space}}} \llbracket |w|^2 \rrbracket_t d\mathbf{x} + \int_{\mathcal{F}_h^{\text{I}}} |w|^2 d\mathbf{x} - \int_{\mathcal{F}_h^0} |w|^2 d\mathbf{x} \right) \\
&+ \frac{1}{2} \Im \left(\int_{\mathcal{F}_h^{\text{time}}} \llbracket w \nabla_{\mathbf{x}} \bar{w} \rrbracket_{\mathbf{N}} dS + \int_{\partial\Omega \times I} w \partial_{\mathbf{n}_{\mathbf{x}}} \bar{w} dS \right) \quad \forall w \in \mathbf{V}(\mathcal{T}_h).
\end{aligned}$$

□

Proposition 2 (Continuity). *The sesquilinear form $\mathcal{A}(\cdot; \cdot)$ and the antilinear functional $\ell(\cdot)$ are continuous in the following sense: $\forall v, w \in \mathbf{V}(\mathcal{T}_h)$*

$$|\mathcal{A}(v; w)| \leq 2|||v|||_{\text{DG}^+} |||w|||_{\text{DG}}, \quad (3.3a)$$

$$|\ell(v)| \leq \left(2 \|\psi_0\|_{L^2(\mathcal{F}_h^0)}^2 + \left\| \alpha^{\frac{1}{2}} g_D \right\|_{L^2(\mathcal{F}_h^D)}^2 + \left\| \beta^{\frac{1}{2}} g_N \right\|_{L^2(\mathcal{F}_h^N)}^2 + \left\| \vartheta^{-\frac{1}{2}} g_R \right\|_{L^2(\mathcal{F}_h^R)}^2 \right)^{\frac{1}{2}} |||w|||_{\text{DG}^+}. \quad (3.3b)$$

Proof The terms on $\mathcal{F}_h^{\text{space}}$, \mathcal{F}_h^T , \mathcal{F}_h^0 , $\mathcal{F}_h^{\text{time}}$ and \mathcal{F}_h^D are controlled as in [11, Prop. 3.3]. The remaining terms are bounded similarly using Cauchy–Schwarz inequality and the inequality $\delta \leq 1 - \delta < 1$. \square

Theorem 1 (Quasi-optimality). *For any finite-dimensional subspace $\mathbb{V}_{hp}(\mathcal{T}_h)$ of $\mathbf{V}(\mathcal{T}_h)$, there exists a unique solution $\psi_{hp} \in \mathbb{V}_{hp}(\mathcal{T}_h)$ satisfying the variational formulation (2.1). Additionally, the following quasi-optimality bound holds:*

$$|||\psi - \psi_{hp}|||_{\text{DG}} \leq 3 \inf_{v_{hp} \in \mathbb{V}_{hp}(\mathcal{T}_h)} |||\psi - v_{hp}|||_{\text{DG}^+}. \quad (3.4)$$

Moreover, if $g_D = 0$ and $g_N = 0$ (or $\Gamma_D = \emptyset$ and $\Gamma_N = \emptyset$), then

$$|||\psi_{hp}|||_{\text{DG}} \leq \left(2 \|\psi_0\|_{L^2(\mathcal{F}_h^0)}^2 + \left\| \vartheta^{-1/2} g_R \right\|_{L^2(\mathcal{F}_h^R)}^2 \right)^{1/2}. \quad (3.5)$$

Proof Existence and uniqueness of the discrete solution $\psi_{hp} \in \mathbb{V}_{hp}(\mathcal{T}_h)$ of the variational formulation (2.1), and the quasi-optimality bound (3.4) follow directly from Propositions 1–2, the consistency of the variational formulation (2.1) and Lax–Milgram theorem. The continuous dependence on the data (3.5) follows from Proposition 1, and the fact that if $g_D = 0$ and $g_N = 0$ (or $\Gamma_D = \emptyset$ and $\Gamma_N = \emptyset$), the term $\|w\|_{\text{DG}^+}$ on the right-hand side of (3.3b) can be replaced by $\|w\|_{\text{DG}}$. \square

Theorem 1 implies that it is possible to obtain error estimates in the mesh-dependent norm $|||\cdot|||_{\text{DG}}$ by studying the best approximation in $\mathbb{V}_{hp}(\mathcal{T}_h)$ of the exact solution in the $|||\cdot|||_{\text{DG}^+}$ norm. Moreover, according to Proposition 3 below, a priori error estimates can be deduced from the local approximation properties of the space $\mathbb{V}_{hp}(\mathcal{T}_h)$ only, as the $|||\cdot|||_{\text{DG}^+}$ norm can be bounded in terms of volume Sobolev seminorms and norms. The proof of error estimates in mesh-independent norms on the full computational domain for ultra-weak DG methods is a delicate issue; see, e.g., [15, Lemma 1] and [27, §5.4] for related results concerning Trefftz methods for the Helmholtz and the wave equations, respectively.

So far, we have not imposed any restriction on the space–time mesh \mathcal{T}_h . Henceforth, in our analysis we assume:

- **Uniform star-shapedness:** There exists $0 < \rho \leq \frac{1}{2}$ such that, each element $K \in \mathcal{T}_h$ is star-shaped with respect to the ball $B := B_{\rho h_K}(\mathbf{z}_K, s_K)$ centered at $(\mathbf{z}_K, s_K) \in K$ and with radius ρh_K .

- **Local quasi-uniformity in space:** there exists a number $\text{lqu}(\mathcal{T}_h) > 0$ such that $h_{K_x^1} \leq h_{K_x^2} \text{lqu}(\mathcal{T}_h)$ for all $K^1 = K_x^1 \times K_t^1, K^2 = K_x^2 \times K_t^2 \in \mathcal{T}_h$ such that $K^1 \cap K^2$ has positive d -dimensional measure.

The proof of Proposition 3 is a direct consequence of a collection of trace inequalities (see [3, Theorem 1.6.6] and [27, Lemma 2]), which in our space–time setting can be written for any element $K = K_x \times K_t \in \mathcal{T}_h$ as

$$\begin{aligned} \|\varphi\|_{L^2(K_x \times \partial K_t)}^2 &\leq C_{\text{tr}} \left(h_{K_t}^{-1} \|\varphi\|_{L^2(K)}^2 + h_{K_t} \|\partial_t \varphi\|_{L^2(K)}^2 \right) \quad \forall \varphi \in H^1(K_t; L^2(K_x)), \\ \|\varphi\|_{L^2(\partial K_x \times K_t)}^2 &\leq C_{\text{tr}} \left(h_{K_x}^{-1} \|\varphi\|_{L^2(K)}^2 + h_{K_x} \|\nabla_x \varphi\|_{L^2(K)^d}^2 \right) \quad \forall \varphi \in L^2(K_t; H^1(K_x)), \\ \|\nabla_x \varphi\|_{L^2(\partial K_x \times K_t)^d}^2 &\leq C_{\text{tr}} \left(h_{K_x}^{-1} \|\nabla_x \varphi\|_{L^2(K)^d}^2 + h_{K_x} \|D_x^2 \varphi\|_{L^2(K)^{d \times d}}^2 \right) \\ &\quad \forall \varphi \in L^2(K_t; H^2(K_x)), \end{aligned} \quad (3.6)$$

where $D_x^2 \varphi$ is the spatial Hessian of φ , and $C_{\text{tr}} \geq 1$ only depends on the star-shapedness parameter ρ .

Proposition 3 Fix $\delta = \min(\vartheta h_{K_x}, \frac{1}{2})$, and assume that $V \in L^\infty(K)$, $\forall K \in \mathcal{T}_h$. For all $\varphi \in \mathbf{V}(\mathcal{T}_h)$, the following bound holds

$$\begin{aligned} |||\varphi|||_{\text{DG}^+}^2 &\leq \frac{3}{2} C_{\text{tr}} \sum_{K=K_x \times K_t \in \mathcal{T}_h} \left[h_{K_t}^{-1} \|\varphi\|_{L^2(K)}^2 + h_{K_t} \|\partial_t \varphi\|_{L^2(K)}^2 + a_K^2 h_{K_x}^{-1} \|\varphi\|_{L^2(K)}^2 \right. \\ &\quad + (a_K^2 h_{K_x} + b_K^2 h_{K_x}^{-1}) \|\nabla_x \varphi\|_{L^2(K)^d}^2 + b_K^2 h_{K_x} \|D_x^2 \varphi\|_{L^2(K)^{d \times d}}^2 + \left\| \mu^{\frac{1}{2}} \partial_t \varphi \right\|_{L^2(K)}^2 \\ &\quad \left. + \left\| \mu^{\frac{1}{2}} \Delta_x \varphi \right\|_{L^2(K)}^2 + \|V\|_{L^\infty(K)}^2 \left\| \mu^{\frac{1}{2}} \varphi \right\|_{L^2(K)}^2 + \left\| \mu^{-\frac{1}{2}} \varphi \right\|_{L^2(K)}^2 \right], \end{aligned}$$

where

$$\begin{aligned} a_K^2 &:= \max \left\{ \text{ess sup}_{\partial K \cap (\mathcal{F}_h^{\text{time}} \cup \mathcal{F}_h^{\text{D}})} \alpha, \left(\text{ess inf}_{\partial K \cap (\mathcal{F}_h^{\text{time}} \cup \mathcal{F}_h^{\text{N}})} \beta \right)^{-1}, \text{ess sup}_{\partial K \cap \mathcal{F}_h^{\text{R}}} \vartheta \right\}, \\ b_K^2 &:= \max \left\{ \left(\text{ess inf}_{\partial K \cap (\mathcal{F}_h^{\text{time}} \cup \mathcal{F}_h^{\text{D}})} \alpha \right)^{-1}, \text{ess sup}_{\partial K \cap (\mathcal{F}_h^{\text{time}} \cup \mathcal{F}_h^{\text{N}})} \beta, h_{K_x} \right\}. \end{aligned}$$

The factor $\frac{3}{2} C_{\text{tr}}$ appearing in the bound of Proposition 3 is due to the integral terms with arguments $\frac{1}{2} \alpha \|w\|_{\text{N}}^2, \frac{1}{2} \beta^{-1} |\{w\}|^2$ on $\mathcal{F}_h^{\text{time}}$ in the definition (3.1) of the $||| \cdot |||_{\text{DG}^+}$ norm. The volume term $\left\| \mu^{\frac{1}{2}} \mathcal{S} w \right\|_{L^2(K)}^2$ is controlled by the inequality $|\mathbf{y}|_1 \leq \sqrt{n} |\mathbf{y}|_2, \forall \mathbf{y} \in \mathbb{C}^n$.

Remark 4 (Inhomogeneous Schrödinger equation). *The space–time ultra-weak DG variational formulation in (2.1) can be easily extended to approximate the solution to inhomogeneous Schrödinger-type problems with a sufficiently smooth term $f : Q_T \rightarrow \mathbb{C}$ at the right-hand side of the first equation in (1.1); see [26, Ch. 3, § 10] for the well-posedness of such problems. In order to preserve the consistency of the method, it is necessary to add the following term to the antilinear functional $\ell(\cdot)$:*

$$\sum_{K \in \mathcal{T}_h} \int_K f (\overline{v_{hp}} + i\mu \overline{\mathcal{S}v_{hp}}) \, dV.$$

The existence and uniqueness of the discrete solution for any choice of the discrete space $\mathbb{V}_{hp}(\mathcal{T}_h)$, as well as the quasi-optimality estimate (3.4), follow from the coercivity and continuity of the sesquilinear form $\mathcal{A}(\cdot; \cdot)$ on the continuous space $\mathbb{V}(\mathcal{T}_h)$ in Propositions 1 and 2, together with the consistency of the method. Thus, optimal convergence rates can be proven for the full polynomial space as in Sect. 4.2, since this space provides a good enough approximation of any sufficiently smooth solution. On the other hand, the quasi-Trefftz space introduced in Sect. 4.3 would require some adjustments in order to approximate the solution of an inhomogeneous problem.

Remark 5 (Energy dissipation). *It is well known that the Schrödinger equation (1.1) with homogeneous Dirichlet and/or Neumann boundary conditions and $\Gamma_R = \emptyset$ preserves the energy (or probability) functional $\mathcal{E}(t; \psi) := \frac{1}{2} \int_{\Omega} |\psi(\mathbf{x}, t)|^2 \, d\mathbf{x}$, i.e., $\frac{d}{dt} \mathcal{E}(t; \psi) = 0$.*

The proposed DG method is dissipative, but the energy loss can be quantified in terms of the local least squares error, the initial condition error, the jumps of the solution on the mesh skeleton, and the error on $\mathcal{F}_h^D \cup \mathcal{F}_h^N$ due to the weak imposition of the boundary conditions. More precisely, for $g_D = 0$, $g_N = 0$ and $\mathcal{F}_h^R = \emptyset$, the discrete solution to (2.1) satisfies

$$\mathcal{E}(0; \psi_0) - \mathcal{E}(T; \psi_{hp}) = \mathcal{E}_{loss} := \delta\mathcal{E} + \frac{1}{2} \|\psi_0 - \psi_{hp}\|_{\mathcal{F}_h^0}^2,$$

where

$$\begin{aligned} \delta\mathcal{E} := & \sum_{K \in \mathcal{T}_h} \left\| \mu^{\frac{1}{2}} \mathcal{S}\psi_{hp} \right\|_{L^2(K)}^2 + \frac{1}{2} \|\llbracket \psi_{hp} \rrbracket_t\|_{L^2(\mathcal{F}_h^{\text{space}})}^2 + \frac{1}{2} \left(\left\| \alpha^{\frac{1}{2}} \psi_{hp} \right\|_{L^2(\mathcal{F}_h^D)}^2 \right. \\ & \left. + \left\| \beta^{\frac{1}{2}} \partial_{\mathbf{n}_x} \psi_{hp} \right\|_{L^2(\mathcal{F}_h^N)}^2 + \left\| \alpha^{\frac{1}{2}} \llbracket \psi_{hp} \rrbracket_{\mathbf{N}} \right\|_{L^2(\mathcal{F}_h^{\text{time}})_d}^2 + \left\| \beta^{\frac{1}{2}} \llbracket \nabla_{\mathbf{x}} \psi_{hp} \rrbracket_{\mathbf{N}} \right\|_{L^2(\mathcal{F}_h^{\text{time}})}^2 \right). \end{aligned}$$

This follows from the definition of the $\|\cdot\|_{\text{DG}}$ norm of the solution ψ_{hp} , the coercivity of the sesquilinear form $\mathcal{A}(\cdot; \cdot)$, the definition of the antilinear functional $\ell(\cdot)$ and simple algebraic manipulations; see [11, Rem. 3.6].

4 Discrete spaces and error estimates

In this section we prove a priori h -convergence estimates on the $||| \cdot |||_{\text{DG}^+}$ norm of the error for some discrete polynomial spaces. In particular, for each element $K \in \mathcal{T}_h$, we consider two different polynomial spaces: the space $\mathbb{P}^p(K)$ of polynomials of degree p on K , and a quasi-Trefftz subspace $\mathbb{QT}^p(K) \subset \mathbb{P}^p(K)$ with much smaller dimension, i.e., $\dim(\mathbb{QT}^p(K)) \ll \dim(\mathbb{P}^p(K))$ (see Proposition 5 below). A polynomial Trefftz space for the case of zero potential V has been studied in [12]. We denote the local dimensions $n_{d+1,p} := \dim(\mathbb{QT}^p(K))$ and $r_{d+1,p} := \dim(\mathbb{P}^p(K))$ in dependence of the space dimension d of the problem and the polynomial degree p , but independent of the element K . For simplicity, we only describe the case where the same polynomial degree is chosen in every element; the general case can easily be studied.

4.1 Multi-index notation and preliminary results

We use the standard multi-index notation for partial derivatives and monomials, adapted to the space–time setting: for $\mathbf{j} = (j_{\mathbf{x}}, j_t) = (j_{x_1}, \dots, j_{x_d}, j_t) \in \mathbb{N}_0^{d+1}$,

$$\begin{aligned} \mathbf{j}! &:= j_{x_1}! \cdots j_{x_d}! j_t!, & |\mathbf{j}| &:= |\mathbf{j}_{\mathbf{x}}| + j_t := j_{x_1} + \cdots + j_{x_d} + j_t, \\ D^{\mathbf{j}} f &:= \partial_{x_1}^{j_{x_1}} \cdots \partial_{x_d}^{j_{x_d}} \partial_t^{j_t} f, & \mathbf{x}^{\mathbf{j}_{\mathbf{x}}} t^{j_t} &:= x_1^{j_{x_1}} \cdots x_d^{j_{x_d}} t^{j_t}. \end{aligned}$$

We also recall the definition and approximation properties of multivariate Taylor polynomials, which constitute the basis of our error analysis. On an open and bounded set $\Upsilon \subset \mathbb{R}^{d+1}$, the Taylor polynomial of order $m \in \mathbb{N}$ (and degree $m-1$), centered at $(\mathbf{z}, s) \in \Upsilon$, of a function $\varphi \in \mathcal{C}^{m-1}(\Upsilon)$ is defined as

$$T_{(\mathbf{z},s)}^m[\varphi](\mathbf{x}, t) := \sum_{|\mathbf{j}| < m} \frac{1}{\mathbf{j}!} D^{\mathbf{j}} \varphi(\mathbf{z}, s) (\mathbf{x} - \mathbf{z})^{\mathbf{j}_{\mathbf{x}}} (t - s)^{j_t}.$$

If $\varphi \in \mathcal{C}^m(\Upsilon)$ and the segment $[(\mathbf{z}, s), (\mathbf{x}, t)] \subset \Upsilon$, the Lagrange's form of the Taylor remainder (see [4, Corollary 3.19]) is bounded as follows:

$$\begin{aligned} \left| \varphi(\mathbf{x}, t) - T_{(\mathbf{z},s)}^m[\varphi](\mathbf{x}, t) \right| &\leq |\varphi|_{\mathcal{C}^m(\Upsilon)} \sum_{|\mathbf{j}|=m} \frac{1}{\mathbf{j}!} |(\mathbf{x} - \mathbf{z})^{\mathbf{j}_{\mathbf{x}}} (t - s)^{j_t}| \\ &\leq \frac{(d+1)^{\frac{m}{2}}}{m!} h_{\Upsilon}^m |\varphi|_{\mathcal{C}^m(\Upsilon)}, \end{aligned}$$

where h_{Υ} is the diameter of Υ . In particular, if Υ is star-shaped with respect to (\mathbf{z}, s) , then the following estimate is obtained

$$\left\| \varphi(\mathbf{x}, t) - T_{(\mathbf{z},s)}^m[\varphi](\mathbf{x}, t) \right\|_{L^2(\Upsilon)} \leq \frac{(d+1)^{\frac{m}{2}} |\Upsilon|^{\frac{1}{2}}}{m!} h_{\Upsilon}^m |\varphi|_{\mathcal{C}^m(\Upsilon)},$$

which, together with the well-known identity (see [3, Prop. (4.1.17)]) $D^j T_{(\mathbf{z},s)}^m [\varphi] = T_{(\mathbf{z},s)}^{m-|j|} [D^j \varphi]$, $|j| < m$, gives the estimate

$$\left| \varphi - T_{(\mathbf{z},s)}^m [\varphi] \right|_{H^r(\Upsilon)} \leq \binom{d+r}{d}^{\frac{1}{2}} \frac{(d+1)^{\frac{m-r}{2}} |\Upsilon|^{\frac{1}{2}}}{(m-r)!} h_{\Upsilon}^{m-r} |\varphi|_{\mathcal{C}^m(\Upsilon)} \quad r < m, \quad \forall \varphi \in \mathcal{C}^m(\Upsilon). \quad (4.1)$$

The Bramble–Hilbert lemma provides an estimate for the error of the averaged Taylor polynomial, see [9] and [3, Thm. 4.3.8].

Lemma 1 (Bramble–Hilbert). *Let $\Upsilon \subset \mathbb{R}^{d+1}$, $1 \leq d \in \mathbb{N}$, be an open and bounded set with diameter h_{Υ} , star-shaped with respect to the ball $B := B_{\rho h_{\Upsilon}}(\mathbf{z}, s)$ centered at $(\mathbf{z}, s) \in \Upsilon$ and with radius ρh_{Υ} , for some $0 < \rho \leq \frac{1}{2}$. If $\varphi \in H^m(\Upsilon)$, the averaged Taylor polynomial of order m (and degree $m - 1$) defined as*

$$\mathcal{Q}^m[\varphi](\mathbf{x}, t) := \frac{1}{|B|} \int_B T_{(\mathbf{z},s)}^m[\varphi](\mathbf{x}, t) \, dV(\mathbf{z}, s),$$

satisfies the following error bound for all $s < m$

$$\left| \varphi - \mathcal{Q}^m[\varphi] \right|_{H^s(\Upsilon)} \leq C_{d,m,\rho} h_{\Upsilon}^{m-s} |\varphi|_{H^m(\Upsilon)} \leq 2 \binom{d+s}{d} \frac{(d+1)^{m-s}}{(m-s-1)!} \frac{h_{\Upsilon}^{m-s}}{\rho^{\frac{d+1}{2}}} |\varphi|_{H^m(\Upsilon)}.$$

A sharp bound on $C_{d,m,\rho} > 0$ is given in [9, p. 986] in dependence of d , s , m and ρ , and the second bound is proven in [27, Lemma 1].

4.2 Full polynomial space

In next theorem, we derive a priori error estimates for the DG formulation (2.1) for the space of elementwise polynomials

$$\mathbb{V}_{hp}(\mathcal{T}_h) = \prod_{K \in \mathcal{T}_h} \mathbb{P}^p(K). \quad (4.2)$$

Theorem 2 *Let $p \in \mathbb{N}$, fix δ as in Proposition 3 and assume that $V \in L^\infty(Q_T)$. Let $\psi \in \mathbf{V}(\mathcal{T}_h) \cap H^{p+1}(\mathcal{T}_h)$ be the exact solution of (1.1) and $\psi_{hp} \in \mathbb{V}_{hp}(\mathcal{T}_h)$ be the solution to the variational formulation (2.1) with $\mathbb{V}_{hp}(\mathcal{T}_h)$ given by (4.2). Set the volume penalty function and the stabilization functions as*

$$\min \left\{ h_{K_t}^2, h_{K_x}^2 \right\} \leq \mu|_K \leq \max \left\{ h_{K_t}^2, h_{K_x}^2 \right\},$$

$$\alpha|_F = \frac{1}{h_{F_x}} \quad \forall F \subset \mathcal{F}_h^{\text{time}} \cup \mathcal{F}_h^{\text{D}}, \quad \beta|_F = h_{F_x} \quad \forall F \subset \mathcal{F}_h^{\text{time}} \cup \mathcal{F}_h^{\text{N}},$$

where

$$\begin{cases} h_{F_x} = h_{K_x} & \text{if } F \subset \partial K \cap (\mathcal{F}_h^D \cup \mathcal{F}_h^N), \\ \min\{h_{K_x^1}, h_{K_x^2}\} \leq h_{F_x} \leq \max\{h_{K_x^1}, h_{K_x^2}\} & \text{if } F = K^1 \cap K^2 \subset \mathcal{F}_h^{\text{time}}, \end{cases}$$

then the following estimate holds

$$\begin{aligned} |||\psi - \psi_{hp}|||_{\text{DG}} &\leq 3\sqrt{6C_{\text{tr}}}\rho^{-\frac{p+1}{2}} \frac{(d+1)^{p+1}}{p!} \sum_{K=K_x \times K_t \in \mathcal{T}_h} \left[h_{K_t}^{-\frac{1}{2}} h_K^{p+1} \right. \\ &\quad + p h_{K_t}^{\frac{1}{2}} h_K^p + \text{lqu}(\mathcal{T}_h) \left(h_{K_x}^{-1} h_K^{p+1} + 2p h_K^p + \frac{(p-1)p}{2} \left(\frac{d+2}{d+1} \right) h_{K_x} h_K^{p-1} \right) \\ &\quad + p \max\{h_{K_x}, h_{K_t}\} h_K^p + \frac{(p-1)p}{2} \left(\frac{d+2}{d+1} \right) \max\{h_{K_x}, h_{K_t}\} h_K^{p-1} \\ &\quad \left. + \|V\|_{L^\infty(K)} \max\{h_{K_x}, h_{K_t}\} h_K^{p+1} + \min\{h_{K_x}^{-1}, h_{K_t}^{-1}\} h_K^{p+1} \right] |\psi|_{H^{p+1}(K)}. \end{aligned}$$

Moreover, if $h_{K_x} \simeq h_{K_t}$ for all $K \in \mathcal{T}_h$, there exists a positive constant C independent of the element sizes h_{K_x}, h_{K_t} , but depending on the degree p , the $L^\infty(Q_T)$ norm of V , the trace inequality constant C_{tr} in (3.6), the local quasi-uniformity parameter $\text{lqu}(\mathcal{T}_h)$ and the star-shapedness parameter ρ such that

$$|||\psi - \psi_{hp}|||_{\text{DG}} \leq C \sum_{K \in \mathcal{T}_h} h_K^p |\psi|_{H^{p+1}(K)}.$$

Proof The proof follows from the choice of the volume penalty function μ and the stabilization functions α, β , the quasi-optimality bound (3.4), Proposition 3, the inequality $\sqrt{|\nabla v|_1} \leq \sum_{i=1}^N \sqrt{|v_i|} \forall v \in \mathbb{R}^N$, the fact that $\mathcal{Q}^{p+1}[\psi|_K] \in \mathbb{V}_{hp}(K)$ for all elements $K \in \mathcal{T}_h$, and the Bramble-Hilbert Lemma 1. \square

4.3 Quasi-Trefftz spaces

We now introduce a polynomial quasi-Trefftz space. Let $p \in \mathbb{N}$ and assume that $V \in \mathcal{C}^{p-2}(K)$. For each $K \in \mathcal{T}_h$ we define the following local polynomial quasi-Trefftz space:

$$\mathbb{QT}^p(K) := \left\{ q_p \in \mathbb{P}^p(K) : D^j S q_p(\mathbf{x}_K, t_K) = 0, |j| \leq p-2 \right\}, \quad (4.3)$$

for some point (\mathbf{x}_K, t_K) in K . We consider the following global discrete space

$$\mathbb{V}_{hp}(\mathcal{T}_h) = \prod_{K \in \mathcal{T}_h} \mathbb{QT}^p(K). \quad (4.4)$$

For all $\mathbf{j} \in \mathbb{N}^{d+1}$, if $V \in \mathcal{C}^{|\mathbf{j}|}(K)$ and $f \in \mathcal{C}^{|\mathbf{j}|+2}(K)$, then by the multi-index Leibniz product rule for multivariate functions we have

$$\begin{aligned} D^{\mathbf{j}} S f(\mathbf{x}_K, t_K) = & i D^{\mathbf{j}_x, \mathbf{j}_t+1} f(\mathbf{x}_K, t_K) + \frac{1}{2} \sum_{\ell=1}^d D^{\mathbf{j}_x+2\mathbf{e}_\ell, \mathbf{j}_t} f(\mathbf{x}_K, t_K) \\ & - \sum_{\mathbf{z} \leq \mathbf{j}} \binom{\mathbf{j}}{\mathbf{z}} D^{\mathbf{j}-\mathbf{z}} V(\mathbf{x}_K, t_K) D^{\mathbf{z}} f(\mathbf{x}_K, t_K), \end{aligned} \quad (4.5)$$

where $\{\mathbf{e}_\ell\}_{\ell=1}^d \subset \mathbb{R}^d$ is the canonical basis,

$$\binom{\mathbf{j}}{\mathbf{z}} = \frac{\mathbf{j}!}{\mathbf{z}!(\mathbf{j}-\mathbf{z})!}, \quad \text{and} \quad \mathbf{j} \leq \mathbf{z} \Leftrightarrow j_{x_i} \leq z_{x_i} \quad (1 \leq i \leq d) \text{ and } j_t \leq z_t.$$

The next proposition is the key ingredient to prove optimal convergence rates in Theorem 3 for the DG method (2.1) when $\mathbb{V}_{hp}(\mathcal{T}_h)$ is chosen as the quasi-Trefftz polynomial space defined in (4.3).

Proposition 4 *Let $p \in \mathbb{N}$ and $K \in \mathcal{T}_h$. Assume that $V \in \mathcal{C}^{\max\{p-2,0\}}(K)$ and $\psi \in \mathcal{C}^p(K)$ satisfies $S\psi = 0$ in K , then the Taylor polynomial $T_{(\mathbf{x}_K, t_K)}^{p+1}[\psi] \in \mathbb{Q}\mathbb{T}^p(K)$.*

Proof By the definition of the Taylor polynomial, $T_{(\mathbf{x}_K, t_K)}^{p+1}[\psi] \in \mathbb{P}^p(K)$. Therefore, it only remains to show that $D^{\mathbf{j}} S T_{(\mathbf{x}_K, t_K)}^{p+1}[\psi](\mathbf{x}_K, t_K) = 0$ for all $|\mathbf{j}| \leq p-2$. Taking $f = T_{(\mathbf{x}_K, t_K)}^{p+1}[\psi]$ in (4.5), all the derivatives of $T_{(\mathbf{x}_K, t_K)}^{p+1}[\psi]$ at (\mathbf{x}_K, t_K) that appear in (4.5) are at most of total order $|\mathbf{j}| + 2 \leq p$, so they coincide with the corresponding derivatives of ψ . Furthermore, since $S\psi = 0$, then

$$D^{\mathbf{j}} S T_{(\mathbf{x}_K, t_K)}^{p+1}[\psi](\mathbf{x}_K, t_K) = D^{\mathbf{j}} S \psi(\mathbf{x}_K, t_K) = 0,$$

which completes the proof. \square

Proposition 4 allows for the use of the Taylor error bound (4.1) in the analysis of the quasi-Trefftz DG scheme.

Theorem 3 *Let $p \in \mathbb{N}$, fix δ as in Proposition 3 and assume that $V \in L^\infty(Q_T) \cap \mathcal{C}^{\max\{p-2,0\}}(\mathcal{T}_h)$. Let $\psi \in \mathbf{V}(\mathcal{T}_h) \cap \mathcal{C}^{p+1}(\mathcal{T}_h)$ be the exact solution of (1.1) and $\psi_{hp} \in \mathbb{V}_{hp}(\mathcal{T}_h)$ be the solution to the variational formulation (2.1) with $\mathbb{V}_{hp}(\mathcal{T}_h)$ given by (4.4). Set the volume penalty function μ and the stabilization functions α, β as in Theorem 2. Then, the following estimate holds*

$$|||\psi - \psi_{hp}|||_{\text{DG}} \leq \frac{3}{2} \sqrt{6C_{\text{tr}}} |Q_T|^{\frac{1}{2}} \frac{(d+1)^{\frac{p+1}{2}}}{(p+1)!} \sum_{K=K_x \times K_t \in \mathcal{T}_h} \left[h_{K_t}^{-\frac{1}{2}} h_K^{p+1} \right]$$

$$\begin{aligned}
& + (p+1)h_{K_i}^{\frac{1}{2}}h_K^p + lqu(\mathcal{T}_h) \left(h_{K_x}^{-1}h_K^{p+1} + 2(p+1)h_K^p + p(p+1) \left(\frac{d+2}{2(d+1)} \right)^{\frac{1}{2}} h_{K_x}h_K^{p-1} \right) \\
& + (p+1) \max\{h_{K_x}, h_{K_i}\}h_K^p + p(p+1) \left(\frac{d+2}{2(d+1)} \right)^{\frac{1}{2}} \max\{h_{K_x}, h_{K_i}\}h_K^{p-1} \\
& + \|V\|_{C^0(K)} \max\{h_{K_x}, h_{K_i}\}h_K^{p+1} + \min\{h_{K_x}^{-1}, h_{K_i}^{-1}\}h_K^{p+1} \Big] |\psi|_{C^{p+1}(K)}.
\end{aligned}$$

Moreover, if $h_{K_x} \simeq h_{K_i}$ for all $K \in \mathcal{T}_h$, there exists a positive constant C independent of the mesh size h , but depending on the degree p , the $L^\infty(Q_T)$ norm of V , the trace inequality constant C_{tr} in (3.6), the local quasi-uniformity parameter $lqu(\mathcal{T}_h)$ and the measure of the space-time domain Q_T such that

$$|||\psi - \psi_{hp}|||_{\text{DG}} \leq C \sum_{K \in \mathcal{T}_h} h_K^p |\psi|_{C^{p+1}(K)}.$$

Proof The proof follows from the choice of the volume penalty function μ and the stabilization functions α , β , the quasi-optimality bound (3.4), bound (3), the inequality $\sqrt{|\mathbf{v}|_1} \leq \sum_{i=1}^N \sqrt{|v_i|} \ \forall \mathbf{v} \in \mathbb{R}^N$, Proposition 4, and the estimate (4.1). \square

The a priori error estimate in Theorem 3 requires stronger regularity assumptions on ψ than Theorem 2 (namely $\psi \in C^{p+1}(\mathcal{T}_h)$ instead of $\psi \in H^{p+1}(\mathcal{T}_h)$) due to the fact that $\mathbb{QT}^p(K)$ is tailored to contain the Taylor polynomial $T_{(\mathbf{x}_K, t_K)}^{p+1}[\psi]$, but in general it does not contain the averaged Taylor polynomial $\mathcal{Q}^{p+1}[\psi]$.

Remark 6 (Non-polynomial spaces) *Optimal h -convergence estimates can also be derived for non-polynomial spaces, by requiring the local space $\mathbb{V}_{hp}(K)$ to contain an element whose Taylor polynomial coincides with that of the exact solution. This is the approach in [11] for the Trefftz space of complex exponential wave functions for the Schrödinger equation with piecewise-constant potential.*

4.3.1 Basis functions and dimension

So far, we have not specified the dimension and a basis for the space $\mathbb{QT}^p(K)$, which is the aim of this section.

Recalling that $r_{d,p} = \dim(\mathbb{P}^p(\mathbb{R}^d)) = \binom{p+d}{d}$, let $\{\widehat{m}_\alpha\}_{\alpha=1}^{r_{d,p}}$ and $\{\widetilde{m}_\beta\}_{\beta=1}^{r_{d,p-1}}$ be bases of $\mathbb{P}_p(\mathbb{R}^d)$ and $\mathbb{P}_{p-1}(\mathbb{R}^d)$, respectively. We define

$$n_{d+1,p} := r_{d,p} + r_{d,p-1} = \binom{p+d}{d} + \binom{p+d-1}{d} = \frac{(p+d-1)!(2p+d)}{d!p!},$$

and the following $n_{d+1,p}$ elements of $\mathbb{QT}^p(K)$

$$\left\{ b_J \in \mathbb{QT}^p(K) : \begin{cases} b_J(\mathbf{x}_K^{(1)}, \cdot) = \widehat{m}_J \text{ and } \partial_{x_1} b_J(\mathbf{x}_K^{(1)}, \cdot) = 0 & \text{if } J \leq r_{d,p} \\ b_J(\mathbf{x}_K^{(1)}, \cdot) = 0 \text{ and } \partial_{x_1} b_J(\mathbf{x}_K^{(1)}, \cdot) = \widetilde{m}_{J-r_{d,p}} & \text{if } r_{d,p} < J \leq n_{d+1,p} \end{cases} \right\}, \quad (4.6)$$

where $g\left(\mathbf{x}_K^{(1)}, \cdot\right)$ denotes the restriction of $g : K \rightarrow \mathbb{C}$ to $x_1 = \mathbf{x}_K^{(1)}$, where $\mathbf{x}_K^{(1)}$ is the first component of $\mathbf{x}_K \in \mathbb{R}^d$.

Any element $q_p \in \mathbb{Q}\mathbb{T}^p(K)$ can be expressed in the scaled monomial basis as

$$q_p(\mathbf{x}, t) = \sum_{|\mathbf{j}| \leq p} C_{\mathbf{j}} \left(\frac{\mathbf{x} - \mathbf{x}_K}{h_K} \right)^{\mathbf{j}_x} \left(\frac{t - t_K}{h_K} \right)^{j_t},$$

for some complex coefficients $\{C_{\mathbf{j}}\}_{|\mathbf{j}| \leq p}$. By the conditions $D^{\mathbf{j}} S q_p(\mathbf{x}_K, t_K) = 0$ for all $|\mathbf{j}| \leq p - 2$, in the definition of $\mathbb{Q}\mathbb{T}^p(K)$, we have the following relations between the coefficients

$$\begin{aligned} \frac{i}{h_K} (j_t + 1) C_{\mathbf{j}_x, j_t+1} + \frac{1}{2h_K^2} \sum_{\ell=1}^d (j_{x_\ell} + 1)(j_{x_\ell} + 2) C_{\mathbf{j}_x+2\mathbf{e}_\ell, j_t}^J \\ - \sum_{\mathbf{z} \leq \mathbf{j}} \frac{h_K^{|\mathbf{j}|-|\mathbf{z}|}}{(\mathbf{j} - \mathbf{z})!} D^{\mathbf{j}-\mathbf{z}} V(\mathbf{x}_K, t_K) C_{\mathbf{z}}^J = 0, \end{aligned}$$

which can be rewritten as

$$\begin{aligned} C_{\mathbf{j}_x+2\mathbf{e}_1, j_t} = \frac{1}{(j_{x_1} + 1)(j_{x_1} + 2)} \left(-2ih_K(j_t + 1) C_{\mathbf{j}_x, j_t+1}^J \right. \\ \left. - \sum_{\ell=2}^d (j_{x_\ell} + 1)(j_{x_\ell} + 2) C_{\mathbf{j}_x+2\mathbf{e}_\ell, j_t}^J + 2 \sum_{\mathbf{z} \leq \mathbf{j}} \frac{h_K^{|\mathbf{j}|-|\mathbf{z}|+2}}{(\mathbf{j} - \mathbf{z})!} D^{\mathbf{j}-\mathbf{z}} V(\mathbf{x}_K, t_K) C_{\mathbf{z}}^J \right). \end{aligned} \quad (4.7)$$

The conditions imposed in (4.6) on the restriction of b_J to $x_1 = \mathbf{x}_K^{(1)}$ fix the coefficients of their expansion for all \mathbf{j} with $j_{x_1} \in \{0, 1\}$. In Figs. 1 and 2, we illustrate how the coefficients that are not immediately determined by the conditions in (4.6) (i.e., those for $j_{x_1} \geq 2$) are uniquely defined and can be computed for the $(1 + 1)$ - and $(2 + 1)$ -dimensional cases using the recurrence relation (4.7).

Proposition 5 *The set of functions $\{b_J\}_{J=1}^{n_{d+1,p}}$ defined in (4.6) are a basis for the space $\mathbb{Q}\mathbb{T}^p(K)$. Therefore,*

$$\begin{aligned} \dim(\mathbb{Q}\mathbb{T}^p(K)) = n_{d+1,p} = \frac{(p + d - 1)!(2p + d)}{d!p!} \\ = \mathcal{O}_{p \rightarrow \infty}(p^d) \ll \dim(\mathbb{P}^p(K)) = \binom{d + 1 + p}{d + 1} = \mathcal{O}_{p \rightarrow \infty}(p^{d+1}). \end{aligned}$$

Proof We first observe that the set of polynomials $\{b_J\}_{J=1}^{n_{d+1,p}}$ is linearly independent due to their restrictions to $x_1 = \mathbf{x}_K^{(1)}$. On the other hand, the relations (4.7), imply that q_p is uniquely determined by its restriction $q_p(\mathbf{x}_K^{(1)}, \cdot)$ and the restriction of its

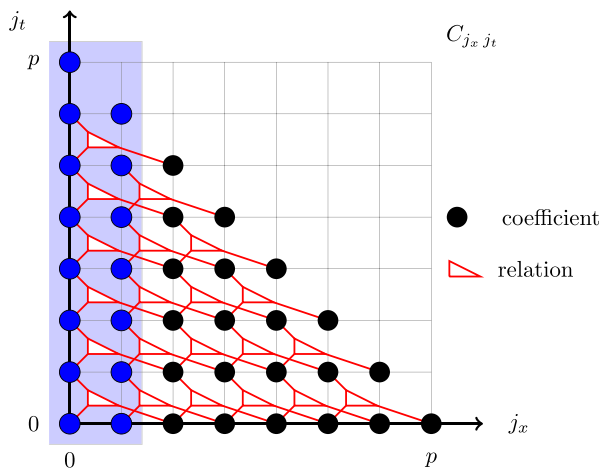
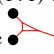


Fig. 1 A representation of the relations defining the coefficients of b_J for the (1+1)-dimensional case. The colored dots in the (j_x, j_t) plane represent the coefficients $C_{j_x j_t}$. Each shape  connects three dots located at the points $(j_x, j_t + 1)$, (j_x, j_t) and $(j_x + 2, j_t)$: this shape represents one of the equations (4.7) which, given $C_{j_x(j_t+1)}$ and $C_{j_x j_t}$, allows to compute $C_{(j_x+2)j_t}$. If the $2p + 1$ values with $j_x \in \{0, 1\}$ (corresponding to the blue nodes in the shaded region) are given, then these relations uniquely determine all the other coefficients, which can be computed sequentially using the relations (4.7) by proceeding left to right in the diagram. In the figure $p = 7$, the number of nodes is $r_{2,p} = 36$, the number of nodes in the shaded region is $n_{2,p} = 15$, the number of relations is $r_{2,p} - n_{2,p} = 21$

derivative $\partial_{x_1} q_p(\mathbf{x}_K^{(1)}, \cdot)$. In addition, there exist some complex coefficients $\{\lambda_s\}_{s=1}^{n_{d+1,p}}$ such that

$$q_p\left(\mathbf{x}_K^{(1)}, \cdot\right) = \sum_{s=1}^{r_{d,p}} \lambda_s \widehat{m}_s(\cdot) = \sum_{s=1}^{r_{d,p}} \lambda_s b_s\left(\mathbf{x}_K^{(1)}, \cdot\right),$$

$$\partial_{x_1} q_p\left(\mathbf{x}_K^{(1)}, \cdot\right) = \sum_{s=r_{d,p}+1}^{n_{d+1,p}} \lambda_s \widetilde{m}_{s-r_{d,p}}(\cdot) = \sum_{s=r_{d,p}+1}^{n_{d+1,p}} \lambda_s \partial_{x_1} b_s\left(\mathbf{x}_K^{(1)}, \cdot\right),$$

whence $q_p = \sum_{s=1}^{n_{d+1,p}} \lambda_s b_s$, which completes the proof. \square

Remark 7 (Quasi-Trefftz basis construction: difference between Schrödinger and wave equations). *The definition of the basis functions b_J in (4.6) can be modified by fixing the restriction of b_J and its partial derivative $\partial_{x_\ell} b_J$ to $x_\ell = \mathbf{x}_K^{(\ell)}$ for any $1 \leq \ell \leq d$. However, it is not possible to assign the values for a given time $t = t_K$, as the order of the time derivative appearing in the Schrödinger equation is lower than the order of the space derivatives. How this affects the basis construction is visible from Fig. 1: the coefficients (the colored dots) can be computed sequentially when all the other coefficients of a relation (the Y-shaped stencil) are known, so it is possible to reach all dots moving left to right, but not moving bottom to top. Imposing the values at a given time is possible for the wave equation, as it is done in [19, §4.4], precisely because in that case time and space derivatives have the same order.*

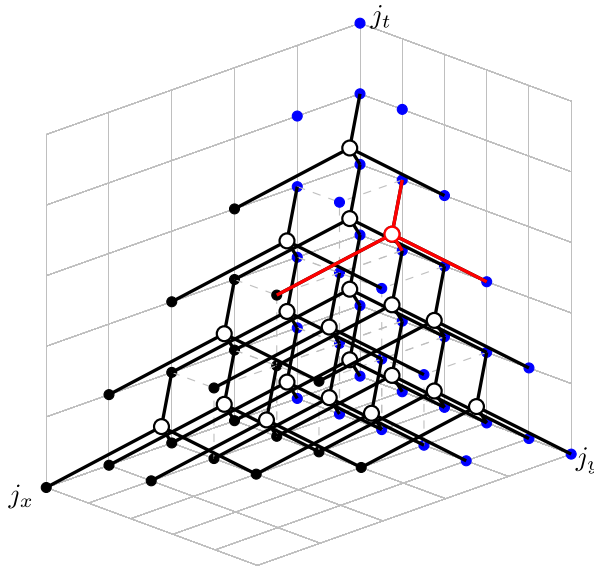


Fig. 2 A representation of the relations defining the coefficients of b_j for the (2+1)-dimensional case. The colored dots in position $\mathbf{j} = (j_x, j_y, j_t)$, $|\mathbf{j}| \leq p$, correspond to the coefficients $C_{j_x j_y j_t}$ (here $p = 5$ and $r_p = 56$). Each white circle is connected by the segments to four nodes and represents one of the equations in (4.7): given $C_{j_x j_y j_t}$, $C_{j_x j_y (j_t+1)}$ and $C_{j_x (j_y+2) j_t}$, it allows to compute $C_{(j_x+2) j_y j_t}$ (the leftmost of the four nodes connected to a given white circle) using (4.7). The red dot exemplifies one of these relations, for $\mathbf{j} = (0, 1, 2)$. Given the $(p+1)^2$ coefficients with $j_x \in \{0, 1\}$ (the blue dots), all other coefficients are uniquely determined

Remark 8 (Constant potential case). *The space $\mathbb{QT}^p(K)$ does not reduce to a Trefftz space for the case of constant potential V . Nonetheless, the pure Trefftz space $\mathbb{T}_p(K)$ defined as*

$$\mathbb{T}_p(K) = \{q_p \in \mathbb{P}^p(K) : Sq_p = 0\},$$

does not possess strong enough approximation properties to guarantee optimal h -convergence. In particular, it does not contain the Taylor polynomial of all local solutions to the Schrödinger equation; for $d = 1$, $p = 1$ and $V = 0$, $\mathbb{T}_p(K) = \text{span}\{1, x\}$; however, $\psi(x, t) = \exp(x + \frac{i}{2}t)$ satisfies $S\psi = 0$, and $T_{(0,0)}^{p+1}[\psi] = 1 + x + \frac{i}{2}t \notin \mathbb{T}_p(K)$.

Remark 9 (Trefftz dimension). *As seen in Proposition 5, the quasi-Trefftz polynomial space has considerably lower dimension than the full polynomial space of the same degree. This “dimension reduction” is common to all Trefftz and quasi-Trefftz schemes. In particular, the dimension $n_{d+1,p}$ of $\mathbb{QT}^p(K)$ is equal to the dimension of the space of harmonic polynomials of degree $\leq p$ in \mathbb{R}^{d+1} , the Trefftz space of complex exponential wave functions for the Schrödinger equation with piecewise-constant potential in [11], the Trefftz and quasi-Trefftz polynomial space for the wave equation in [27, Eqs. (42)–(43)] and [19].*

5 Numerical experiments

In this section we validate the theoretical results regarding the h -convergence of the proposed method, and numerically assess some additional features such as p -convergence and conditioning. Although we do not report the results here, optimal convergence rates of order $\mathcal{O}(h^{p+1})$ are observed for the error in the $L^2(Q_T)$ -norm.

We list some aspects regarding our numerical experiments

- We use Cartesian-product space–time meshes with uniform partitions along each direction, which are a particular case of the situation described in Remark 1.
- We choose (\mathbf{x}_K, t_K) in the definition of the quasi-Trefftz space $\mathbb{QT}^p(K)$ in (4.3) as the center of the element K .
- In all the experiments we consider Dirichlet boundary conditions.
- The linear systems are solved using Matlab's backslash command.
- The quasi-Trefftz basis functions $\{b_J\}_{J=1}^{n_{d+1,p}}$ are constructed by choosing \widehat{m}_J and \widetilde{m}_J in (4.6) as scaled monomials and by computing the remaining coefficients C_J with the relations (4.7).
- In the h -convergence plots, the numbers in the yellow rectangles are the empirical algebraic convergence rates for the quasi-Trefftz version (continuous lines). The dashed lines correspond to the errors obtained for the full polynomial space.

5.1 (1 + 1)-dimensional test cases

We first focus on the (1 + 1)-dimensional case, for which families of explicit solutions are available for some well-known potentials V .

5.1.1 h -convergence

In order to validate the error estimates in Theorems 2 and 3, we consider a series of problems with different potentials V . No significant difference in terms of accuracy between the quasi-Trefftz and the full polynomial versions of the method with the same polynomial degree p (corresponding to different numbers of DOFs $n_{d+1,p}$ and $r_{d+1,p}$, respectively) is observed in all the experiments.

Harmonic oscillator potential ($V(x) = \frac{\omega^2 x^2}{2}$) For this potential, the Schrödinger equation (1.1) models the situation of a quantum harmonic oscillator for an angular frequency $\omega > 0$. On $Q_T = (-3, 3) \times (0, 1)$, we consider the following well-known family of solutions (see, e.g., [13, Sect. 2.3])

$$\psi_n(x, t) = \frac{1}{\sqrt{2^n n!}} \left(\frac{\omega}{\pi}\right)^{1/4} \mathcal{H}_n(\sqrt{\omega}x) \exp\left(-\frac{1}{2}(\omega x^2 + (2n+1)i\omega t)\right) \quad n \in \mathbb{N}, \quad (5.1)$$

where $\mathcal{H}_n(\cdot)$ denotes the n -th physicist's Hermite polynomials as defined in [29, Table 18.3.1, denoted by $H_n(\cdot)$].

In Fig. 3, we present the errors obtained for $\omega = 10$, $n = 2$ and a sequence of Cartesian meshes with uniform partitions and $h_x = h_t = 0.05 \times 2^{-i}$, $i = 0, \dots, 4$.

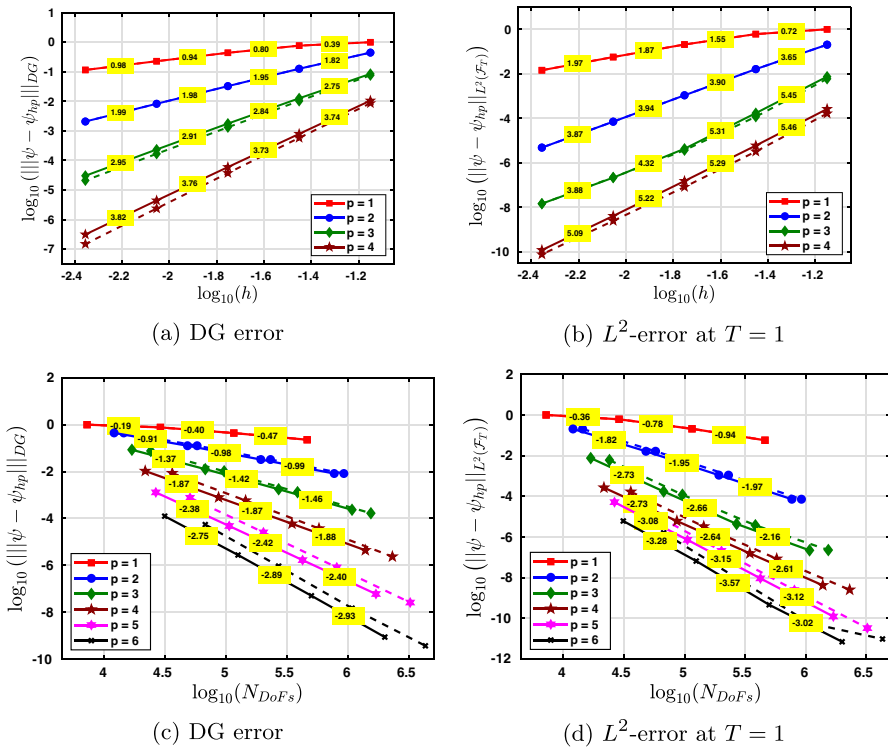


Fig. 3 h -convergence for the $(1 + 1)$ quantum harmonic oscillator problem with potential $(V(x) = 50x^2)$ and exact solution ψ_2 in (5.1). Convergence with respect to the mesh size h (top panels) and the total number of degrees of freedom (bottom panels)

Rates of convergence of order $\mathcal{O}(h^p)$ in the DG norm are observed, as predicted by the error estimate in Theorem 3. A convergence of at least order $\mathcal{O}(h^{p+1})$ is observed for the L^2 -error at the final time, which is faster (by a factor h) than the order that can be deduced from the estimates in Theorems 2 and 3. We have also included the plots for the error decay with respect to the total number of degrees of freedom, where the same h -convergence rates are observed for both versions of the method (see also the p -convergence plot in Fig. 4a for a clearer understanding of the dependence of the error on p).

Due to the fast decay of the exact solution close to the boundary (see Fig. 5 (panel a)), the energy is expected to be preserved. In Fig. 6, we show the evolution of the energy error, and the convergence of the energy loss \mathcal{E}_{loss} to zero for the quasi-Trefftz version. In the latter, rates of order $\mathcal{O}(h^{2p})$ are observed, which follows from Remark 5 and the error estimates in Theorems 2 and 3.

Reflectionless potential ($V(x) = -a^2 \text{sech}^2(ax)$) This potential was studied in [5] as an example of a reflectionless potential. On the space–time domain $Q_T = (-5, 5) \times (0, 1)$, we consider the Schrödinger equation with exact solution (see [13, Problem

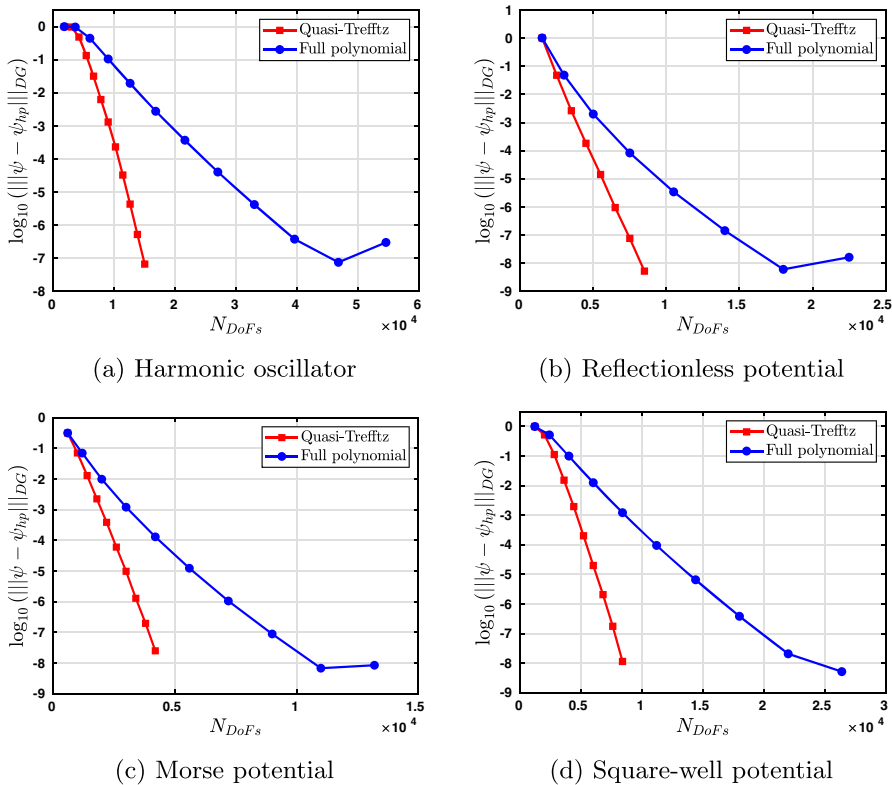


Fig. 4 p -convergence for the coarsest mesh in the $(1 + 1)$ -dimensional problems

2.48])

$$\psi(x, t) = \left(\frac{\sqrt{2}i - a \tanh(ax)}{\sqrt{2}i + a} \right) \exp(i(\sqrt{2}x - t)). \quad (5.2)$$

In Fig. 7, we show the errors obtained for a sequence of meshes with $h_x = 2h_t = 0.2 \times 2^{-i}$, $i = 0, \dots, 4$, and $a = 1$. As in the previous experiment, rates of convergence of order $\mathcal{O}(h^p)$ and $\mathcal{O}(h^{p+1})$ are observed in the DG norm and the L^2 norm at the final time, respectively. The real part of the exact solution is depicted in Fig. 5 (panel b).

Morse potential ($V(x) = D(1 - e^{-\alpha x})^2$) This potential was introduced by Morse in [28] to obtain a quantum-mechanical energy level spectrum of a vibrating, non-rotating diatomic molecule. There, the following family of solutions was presented (see also [6])

$$\psi_{\lambda, n}(x, t) = N(\lambda, n) \xi(x)^{\lambda - n - 1/2} \mathbb{L}_n^{(2\lambda - 2n - 1)}(\xi(x)) \quad (5.3)$$

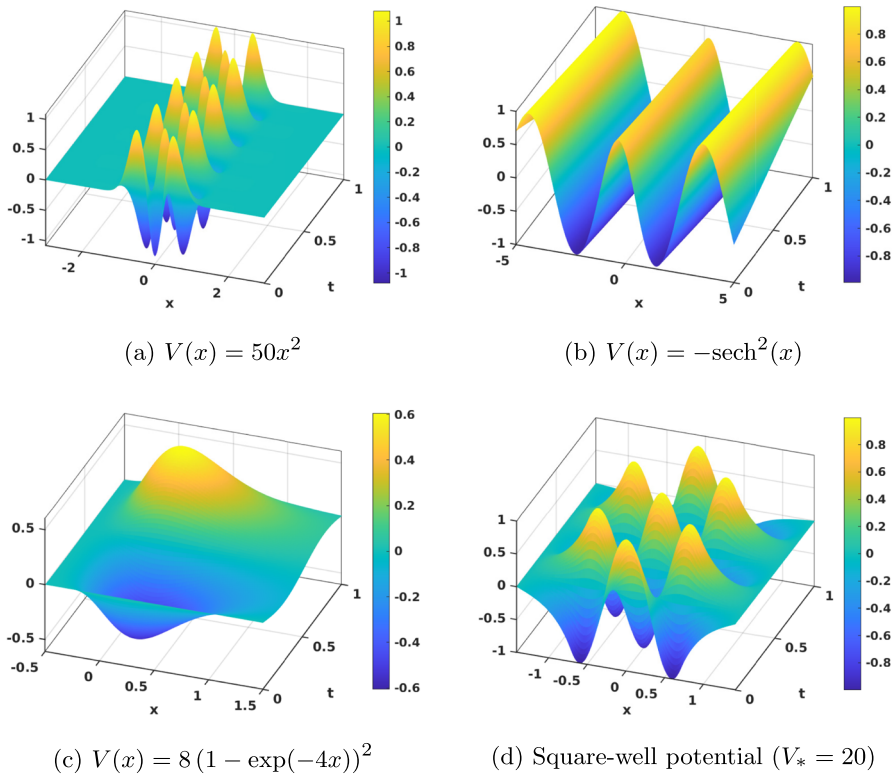


Fig. 5 Real part of the exact solutions for the $(1 + 1)$ -dimensional problems

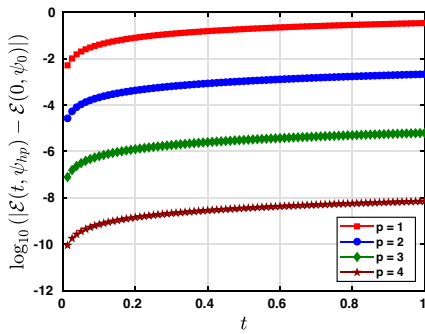
$$\times \exp\left(-\frac{\xi(x)}{2} - it\left[(n + 1/2) - \frac{1}{2\lambda}(n + 1/2)^2\right]\omega_o\right),$$

where $\lfloor \cdot \rfloor$ is the floor function, $n = 0, \dots, \lfloor \lambda - 1/2 \rfloor$, $\mathbb{L}_n^{(\alpha)}$ denote the general associated Laguerre polynomials as defined in [29, Table 18.3.1] and

$$N(\lambda, n) = \left[\frac{(2\lambda - 2n - 1)\Gamma(n + 1)}{\Gamma(2\lambda - n)} \right]^{\frac{1}{2}}, \quad \lambda = \frac{\sqrt{2D}}{\alpha}, \quad \xi(x) = 2\lambda \exp(-\alpha x), \quad \omega_o = \sqrt{2D}\alpha.$$

In Fig. 8, we show the errors obtained for the Morse potential problem with $D = 8$, $\alpha = 4$ and exact solution $\psi_{1,1}$ on the space–time domain $Q_T = (-0.5, 1.5) \times (0, 1)$ for a sequence of meshes with $h_x = h_t = 0.1 \times 2^{-i}$, $i = 0, \dots, 4$. The observed rates of convergence are in agreement with those obtained in the previous experiments. The real part of the exact solution is depicted in Fig. 5 (panel c).

Square-well potential We now consider a problem taken from [11], whose exact solution is not globally smooth. On the space–time domain $Q_T = (-\sqrt{2}, \sqrt{2}) \times (0, 1)$, we consider the Schrödinger equation with homogeneous Dirichlet boundary



(a) Energy error evolution

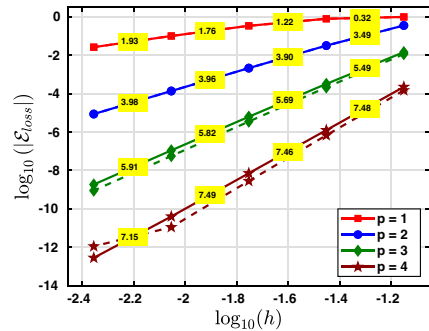
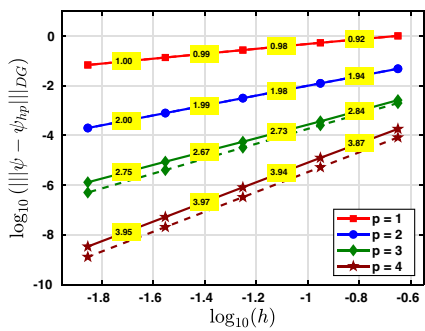
(b) Energy loss at $T = 1$

Fig. 6 Time-evolution of the energy error for the quantum harmonic oscillator problem with potential $(V(x) = 50x^2)$ and exact solution ψ_2 in (5.1)



(a) DG error

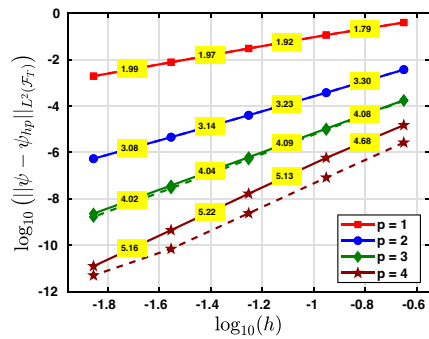
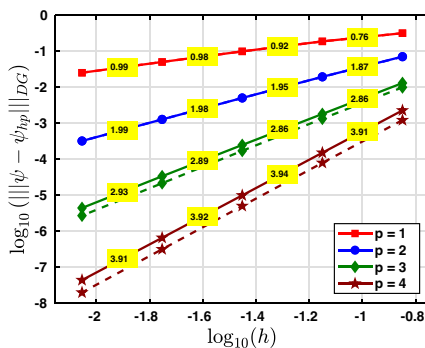
(b) L^2 -error at $T = 1$

Fig. 7 h -convergence for the $(1+1)$ problem with potential $V(x) = -\text{sech}^2(x)$ and exact solution (5.2)



(a) DG error

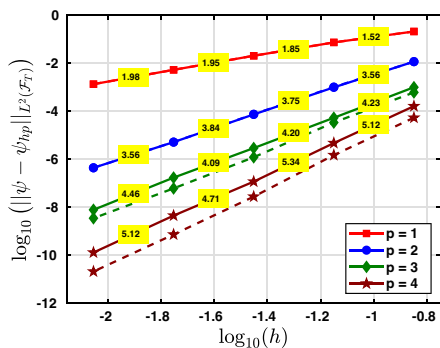
(b) L^2 -error at $T = 1$

Fig. 8 h -convergence for the $(1+1)$ -dimensional problem with Morse potential $V(x) = D(1 - \exp(-\alpha x))^2$ for $D = 8$ and $\alpha = 4$ with exact solution (5.3)

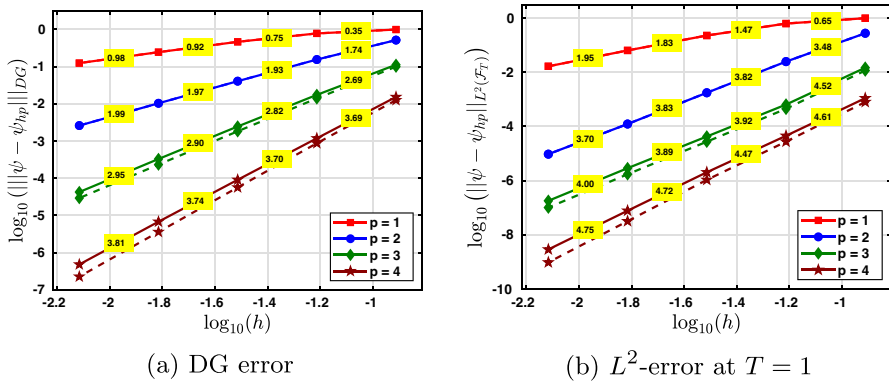


Fig. 9 h -convergence for the (1 + 1)-dimensional problem with the square-well potential $V(x)$ in (5.4)

conditions and the following square-well potential

$$V(x) = \begin{cases} 0 & x \in (-1, 1), \\ V_* & x \in (-\sqrt{2}, \sqrt{2}) \setminus (-1, 1), \end{cases} \quad (5.4)$$

for some fixed $V_* > 0$. The initial condition is taken as an eigenfunction (bound state) of $-\frac{1}{2}\partial_x^2 + V$ on $(-\sqrt{2}, \sqrt{2})$:

$$\psi_0(x) = \begin{cases} \cos(k_*\sqrt{2}x) & x \in (-1, 1), \\ \frac{\cos(k_*)}{\sinh(\sqrt{V_* - k_*^2})} \sinh(\sqrt{V_* - k_*^2}(2 - \sqrt{2}|x|)) & x \in (-\sqrt{2}, \sqrt{2}) \setminus (-1, 1), \end{cases}$$

where k_* is a real root of the function $f(k) := \sqrt{V_* - k^2} - k \tan(k) \tanh(\sqrt{V_* - k^2})$. The solution of the corresponding initial boundary value problem (1.1) is $\psi(x, t) = \psi_0(x) \exp(-ik^2t)$ and belongs to the space $H^{p+1}(\mathcal{T}_h) \cap \mathcal{C}^\infty(I; \mathcal{C}^1(\Omega)) \setminus \mathcal{C}^\infty(I; \mathcal{C}^2(\Omega))$ for all $p \in \mathbb{N}$, provided that \mathcal{T}_h is aligned with the discontinuities of the potential V ; therefore, Theorems 2 and 3 apply. Among the finite set of values k_* for a given V_* , in this experiment we take the largest one, corresponding to faster oscillations in space and time.

In Fig. 9, we show the errors obtained for $V_* = 20$ ($k_* \approx 3.73188$) and a sequence of meshes with $h_t = \sqrt{2}h_x = 0.1 \times 2^{-i}$, $i = 0, \dots, 4$. Optimal convergence in both norms is observed for the errors of the quasi-Trefftz version of the method.

5.1.2 Effect of stabilization and volume penalty terms

In this experiment we are interested in the effect of neglecting some of the terms in the variational formulation (2.1). To do so, we consider the (1 + 1)-dimensional quantum harmonic oscillator problem with exact solution (5.1). In Tables 1 and 2 (quasi-Trefftz space) and Tables 3 and 4 (full polynomial space) we present the errors in the DG norm obtained for the same sequence of meshes and approximation degrees

Table 1 h -convergence for the quasi-Trefftz version applied to the quantum harmonic oscillator problem with potential $V(x) = 50x^2$ and exact solution ψ_2 in (5.1) for different combinations of the stabilization parameters α , β and volume penalty parameter $\mu \neq 0$. Convergences rates are shown in bold

h	$\mu = \max\{h_{K_I}, h_{K_X}\}$		$\alpha = 0, \beta = 0$		$\alpha = \frac{1}{h_{F_X}}, \beta = 0$		$\alpha = 0, \beta = h_{F_X}$	
	$\alpha = \frac{1}{h_{F_X}}, \beta = h_{F_X}$							
	DG error	Rate	DG error	Rate	DG error	Rate	DG error	Rate
$p = 1$								
7.07e-02	1.00e+00	—	9.81e-01	—	1.01e+00	—	1.00e+00	—
3.54e-02	7.67e-01	0.39	4.76e-01	1.04	6.72e-01	0.58	6.53e-01	0.62
1.77e-02	4.40e-01	0.80	2.14e-01	1.15	3.62e-01	0.89	3.40e-01	0.94
8.84e-03	2.29e-01	0.94	1.01e-01	1.08	1.85e-01	0.97	1.70e-01	1.00
4.42e-03	1.16e-01	0.98	4.96e-02	1.03	9.31e-02	0.99	8.49e-02	1.00
$p = 2$								
7.07e-02	4.47e-01	—	2.59e-01	—	2.99e-01	—	4.37e-01	—
3.54e-02	1.27e-01	1.82	6.90e-02	1.91	8.24e-02	1.86	1.20e-01	1.87
1.77e-02	3.28e-02	1.95	1.78e-02	1.96	2.15e-02	1.94	3.05e-02	1.97
8.84e-03	8.29e-03	1.98	4.50e-03	1.98	5.48e-03	1.97	7.68e-03	1.99
4.42e-03	2.08e-03	1.99	1.13e-03	1.99	1.38e-03	1.98	1.93e-03	2.00
$p = 3$								
7.07e-02	8.54e-02	—	5.73e-02	—	5.87e-02	—	8.65e-02	—
3.54e-02	1.27e-02	2.75	8.00e-03	2.84	8.28e-03	2.83	1.27e-02	2.77
1.77e-02	1.77e-03	2.84	1.08e-03	2.89	1.12e-03	2.88	1.75e-03	2.86
8.84e-03	2.35e-04	2.91	1.42e-04	2.93	1.48e-04	2.93	2.32e-04	2.92
4.42e-03	3.04e-05	2.95	1.82e-05	2.96	1.90e-05	2.96	2.99e-05	2.96
$p = 4$								
7.07e-02	1.06e-02	—	9.36e-03	—	9.27e-03	—	1.08e-02	—
3.54e-02	7.93e-04	3.74	6.56e-04	3.84	6.64e-04	3.80	7.95e-04	3.76
1.77e-02	5.97e-05	3.73	4.59e-05	3.84	4.66e-05	3.83	5.94e-05	3.74
8.84e-03	4.42e-06	3.76	3.16e-06	3.86	3.21e-06	3.86	4.39e-06	3.76
4.42e-03	3.13e-07	3.82	2.11e-07	3.90	2.14e-07	3.90	3.11e-07	3.82

as in the previous section, for different combinations of the stabilization terms α , β and the volume penalty parameter μ . Although the proof of well-posedness of the method (2.1) relies on the assumption that α , β and μ are strictly positive, in our numerical experiments, the matrices of the arising linear systems are non-singular and optimal convergence rates are observed even when all these parameters are set to zero. Moreover, the errors obtained when $\alpha = 0$ or $\beta = 0$ are smaller as some terms in the definition (3.1) of $\|\cdot\|_{\text{DG}}$ vanish, while the presence of μ seems to have just a mild effect in the results. Not shown here, similar effects were observed for the error in the $L^2(\mathcal{F}_h^T)$ -norm.

Table 2 h -convergence for the quasi-Trefftz version applied to the quantum harmonic oscillator problem with potential $V(x) = 50x^2$ and exact solution ψ_2 in (5.1) for different combinations of the stabilization parameters α, β and volume penalty parameter $\mu = 0$. Convergences rates are shown in bold

h	$\mu = 0$		$\alpha = 0, \beta = 0$		$\alpha = \frac{1}{h_{F_x}}, \beta = 0$		$\alpha = 0, \beta = h_{F_x}$	
	$\alpha = \frac{1}{h_{F_x}}, \beta = h_{F_x}$							
	DG error	Rate	DG error	Rate	DG error	Rate	DG error	Rate
$p = 1$								
7.07e−02	1.04e+00	—	1.16e+00	—	1.07e+00	—	1.09e+00	—
3.54e−02	7.78e−01	0.43	5.02e−01	1.21	6.84e−01	0.64	6.69e−01	0.70
1.77e−02	4.42e−01	0.81	2.18e−01	1.20	3.64e−01	0.91	3.42e−01	0.97
8.84e−03	2.29e−01	0.95	1.02e−01	1.09	1.85e−01	0.97	1.71e−01	1.00
4.42e−03	1.16e−01	0.99	4.98e−02	1.04	9.32e−02	0.99	8.50e−02	1.01
$p = 2$								
7.07e−02	4.63e−01	—	2.96e−01	—	3.23e−01	—	4.60e−01	—
3.54e−02	1.29e−01	1.84	7.38e−02	2.00	8.58e−02	1.91	1.23e−01	1.90
1.77e−02	3.31e−02	1.97	1.84e−02	2.01	2.19e−02	1.97	3.09e−02	1.99
8.84e−03	8.33e−03	1.99	4.58e−03	2.00	5.54e−03	1.99	7.73e−03	2.00
4.42e−03	2.09e−03	2.00	1.14e−03	2.00	1.39e−03	1.99	1.93e−03	2.00
$p = 3$								
7.07e−02	8.73e−02	—	7.84e−02	—	7.59e−02	—	8.85e−02	—
3.54e−02	1.31e−02	2.74	9.65e−03	3.02	9.72e−03	2.96	1.31e−02	2.76
1.77e−02	1.82e−03	2.85	1.20e−03	3.01	1.23e−03	2.98	1.80e−03	2.86
8.84e−03	2.39e−04	2.92	1.50e−04	3.00	1.55e−04	2.99	2.36e−04	2.93
4.42e−03	3.07e−05	2.96	1.87e−05	3.00	1.95e−05	2.99	3.02e−05	2.97
$p = 4$								
7.07e−02	1.09e−02	—	1.71e−02	—	1.56e−02	—	1.12e−02	—
3.54e−02	7.97e−04	3.77	9.77e−04	4.13	9.60e−04	4.02	7.98e−04	3.81
1.77e−02	6.02e−05	3.73	5.97e−05	4.03	5.98e−05	4.00	5.99e−05	3.73
8.84e−03	4.50e−06	3.74	3.71e−06	4.01	3.74e−06	4.00	4.48e−06	3.74
4.42e−03	3.19e−07	3.82	2.31e−07	4.00	2.34e−07	4.00	3.17e−07	3.82

5.1.3 p -convergence

We now study numerically the p -convergence of the method, i.e., for a fixed space–time mesh \mathcal{T}_h , we study the errors when increasing the polynomial degree p . We consider the $(1 + 1)$ -dimensional problems above with the same parameters and the coarsest meshes for each case. In Fig. 4, we compare the errors obtained for the method with the two choices for the discrete space $\mathbb{V}_{hp}(\mathcal{T}_h)$ analyzed in the previous sections: the full polynomial space (4.2) and the quasi-Trefftz polynomial space (4.4). As expected, for the quasi-Trefftz version we observe exponential decay of the error of order $\mathcal{O}(e^{-bN_{DoFs}})$, where N_{DoFs} denotes the total number of degrees of freedom. As for the full polynomial space, only root-exponential convergence $\mathcal{O}(e^{-c\sqrt{N_{DoFs}}})$ is

Table 3 h -convergence for the full polynomial version applied to the quantum harmonic oscillator problem with potential $V(x) = 50x^2$ and exact solution ψ_2 in (5.1) for different combinations of the stabilization parameters α, β and volume penalty parameter $\mu \neq 0$. Convergences rates are shown in bold

h	$\mu = \max\{h_{K_I}, h_{K_X}\}$		$\alpha = 0, \beta = 0$		$\alpha = \frac{1}{h_{F_X}}, \beta = 0$		$\alpha = 0, \beta = h_{F_X}$	
	$\alpha = \frac{1}{h_{F_X}}, \beta = h_{F_X}$							
	DG error	Rate	DG error	Rate	DG error	Rate	DG error	Rate
$p = 1$								
7.07e-02	1.00e+00	—	9.81e-01	—	1.01e+00	—		
3.54e-02	7.67e-01	0.39	4.76e-01	1.04	6.72e-01	0.58	1.00e+00	—
1.77e-02	4.40e-01	0.80	2.14e-01	1.15	3.62e-01	0.89	3.40e-01	0.94
8.84e-03	2.29e-01	0.94	1.01e-01	1.08	1.85e-01	0.97	1.70e-01	1.00
4.42e-03	1.16e-01	0.98	4.96e-02	1.03	9.31e-02	0.99	8.49e-02	1.00
$p = 2$								
7.07e-02	4.46e-01	—	2.55e-01	—	2.96e-01	—	4.34e-01	—
3.54e-02	1.27e-01	1.81	6.88e-02	1.89	8.22e-02	1.85	1.20e-01	1.86
1.77e-02	3.28e-02	1.95	1.77e-02	1.95	2.15e-02	1.94	3.05e-02	1.97
8.84e-03	8.29e-03	1.98	4.50e-03	1.98	5.48e-03	1.97	7.68e-03	1.99
4.42e-03	2.08e-03	1.99	1.13e-03	1.99	1.38e-03	1.98	1.93e-03	2.00
$p = 3$								
7.07e-02	7.62e-02	—	4.67e-02	—	4.93e-02	—	7.65e-02	—
3.54e-02	1.03e-02	2.89	6.22e-03	2.91	6.68e-03	2.88	1.01e-02	2.92
1.77e-02	1.33e-03	2.96	8.05e-04	2.95	8.71e-04	2.94	1.29e-03	2.97
8.84e-03	1.68e-04	2.98	1.03e-04	2.97	1.11e-04	2.97	1.62e-04	2.99
4.42e-03	2.11e-05	2.99	1.30e-05	2.99	1.41e-05	2.98	2.03e-05	2.99
$p = 4$								
7.07e-02	8.63e-03	—	6.05e-03	—	6.14e-03	—	8.74e-03	—
3.54e-02	5.82e-04	3.89	3.95e-04	3.94	4.10e-04	3.90	5.77e-04	3.92
1.77e-02	3.74e-05	3.96	2.54e-05	3.96	2.66e-05	3.95	3.67e-05	3.97
8.84e-03	2.37e-06	3.98	1.62e-06	3.97	1.69e-06	3.97	2.32e-06	3.99
4.42e-03	1.49e-07	3.99	1.02e-07	3.99	1.07e-07	3.98	1.45e-07	3.99

expected. The superiority of the quasi-Trefftz version is evident in all cases. Exponential convergence of space–time Trefftz and quasi-Trefftz schemes has been observed in several cases [1, 11, 17, 30] but no proof is available yet (differently from the stationary case [16, §3]). In general, for a $(d + 1)$ -dimensional problem, we expect exponential convergence of order $\mathcal{O}(e^{-b\sqrt[d]{N_{DoFs}}})$ and $\mathcal{O}(e^{-c\sqrt[(d+1)]{N_{DoFs}}})$ for the quasi-Trefftz and full polynomial versions, respectively.

5.1.4 Conditioning

We now assess the conditioning of the stiffness matrix. In Fig. 10 we compare the 2-condition number $\kappa_2(\cdot)$ for the stiffness matrix \mathbf{K}_n defined in Remark 1, for the free particle problem $V = 0$ on the space–time domain $Q_T = (0, 1) \times (0, 1)$. We consider

Table 4 h -convergence for the full polynomial version applied to the quantum harmonic oscillator problem with potential $V(x) = 50x^2$ and exact solution ψ_2 in (5.1) for different combinations of the stabilization parameters α, β and volume penalty parameter $\mu = 0$. Convergences rates are shown in bold

h	$\mu = 0$		$\alpha = 0, \beta = 0$		$\alpha = \frac{1}{h_{F_x}}, \beta = 0$		$\alpha = 0, \beta = h_{F_x}$	
	$\alpha = \frac{1}{h_{F_x}}, \beta = h_{F_x}$							
	DG error	Rate	DG error	Rate	DG error	Rate	DG error	Rate
$p = 1$								
7.07e−02	1.04e+00	—	1.16e+00	—	1.07e+00	—	1.09e+00	—
3.54e−02	7.78e−01	0.43	5.02e−01	1.21	6.84e−01	0.64	6.69e−01	0.70
1.77e−02	4.42e−01	0.81	2.18e−01	1.20	3.64e−01	0.91	3.42e−01	0.97
8.84e−03	2.29e−01	0.95	1.02e−01	1.09	1.85e−01	0.97	1.71e−01	1.00
4.42e−03	1.16e−01	0.99	4.98e−02	1.04	9.32e−02	0.99	8.50e−02	1.01
$p = 2$								
7.07e−02	4.63e−01	—	2.93e−01	—	3.22e−01	—	4.57e−01	—
3.54e−02	1.29e−01	1.84	7.36e−02	1.99	8.57e−02	1.91	1.23e−01	1.90
1.77e−02	3.31e−02	1.97	1.84e−02	2.00	2.19e−02	1.97	3.09e−02	1.99
8.84e−03	8.33e−03	1.99	4.58e−03	2.00	5.54e−03	1.98	7.72e−03	2.00
4.42e−03	2.09e−03	2.00	1.14e−03	2.00	1.39e−03	1.99	1.93e−03	2.00
$p = 3$								
7.07e−02	8.09e−02	—	5.42e−02	—	5.54e−02	—	8.19e−02	—
3.54e−02	1.06e−02	2.93	6.74e−03	3.01	7.12e−03	2.96	1.04e−02	2.97
1.77e−02	1.35e−03	2.98	8.41e−04	3.00	9.02e−04	2.98	1.31e−03	3.00
8.84e−03	1.69e−04	2.99	1.05e−04	3.00	1.13e−04	2.99	1.64e−04	3.00
4.42e−03	2.12e−05	3.00	1.31e−05	3.00	1.42e−05	3.00	2.04e−05	3.00
$p = 4$								
7.07e−02	9.27e−03	—	6.96e−03	—	6.94e−03	—	9.48e−03	—
3.54e−02	6.03e−04	3.94	4.27e−04	4.03	4.39e−04	3.98	5.99e−04	3.99
1.77e−02	3.81e−05	3.98	2.66e−05	4.01	2.76e−05	3.99	3.74e−05	4.00
8.84e−03	2.39e−06	3.99	1.66e−06	4.00	1.73e−06	3.99	2.34e−06	4.00
4.42e−03	1.50e−07	4.00	1.04e−07	4.00	1.08e−07	4.00	1.46e−07	4.00

the proposed polynomial quasi-Trefftz space in (4.4), the full polynomial space in (4.2) and the pure Trefftz space of complex exponential wave functions $\mathbb{T}_p(\mathcal{T}_h)$ proposed in [11]. A basis $\{\phi_\ell\}_{\ell=1}^{2p+1} \subset \mathbb{T}_p(\mathcal{T}_h)$ was defined in [11] as

$$\phi_\ell(x, t) = \exp\left(i\left(\kappa_\ell x - \frac{\kappa_\ell^2}{2}t\right)\right), \quad \ell = 1, \dots, 2p + 1. \quad (5.5)$$

We consider two choices for the parameters κ_ℓ : the arbitrary choice used in [11] $\kappa_\ell = -p, \dots, p$, and the choice $\kappa_\ell = 2\pi\ell/h_x$ which makes the basis orthogonal in each element. The conditioning number $\kappa_2(\mathbf{K})$ for the quasi-Trefftz space, the full polynomial space, and the Trefftz space with orthogonal basis asymptotically grows

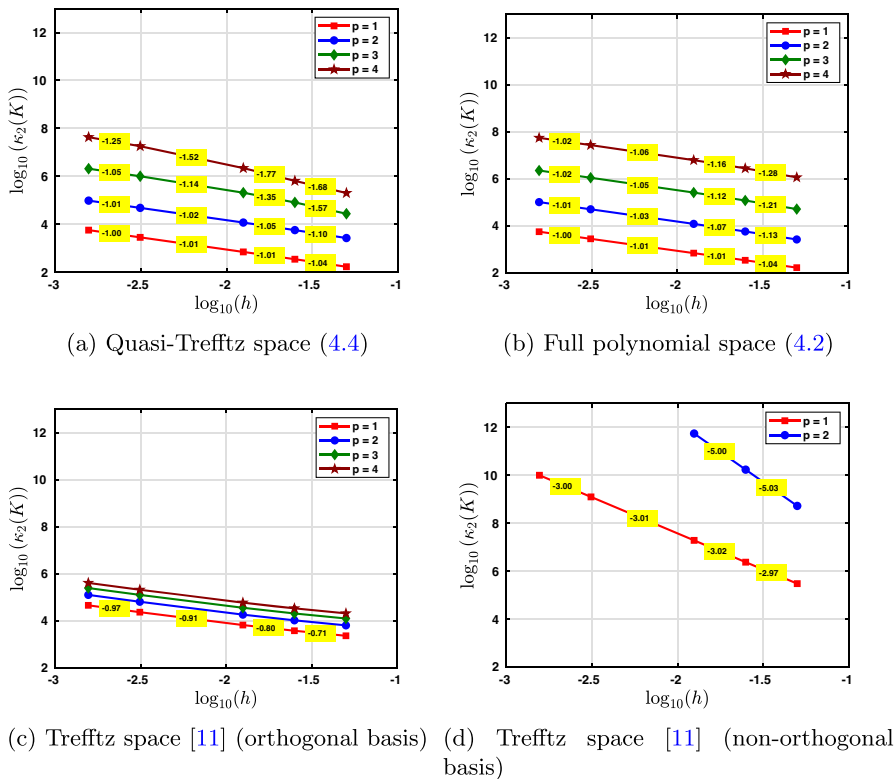


Fig. 10 Conditioning of the stiffness matrix for the DG method with different discrete spaces

as $\mathcal{O}(h^{-1})$ for all $p \in \mathbb{N}$, while for the Trefftz space with a non-orthogonal basis, asymptotically grows as $\mathcal{O}(h^{-(2p+1)})$. Unfortunately, with higher dimensions and non-Cartesian elements, choosing the parameters and directions defining the basis functions $\{\phi_\ell\}$ so as to obtain an orthogonal basis is more challenging.

5.2 (2 + 1)-dimensional test cases

We now present some numerical test for space dimension $d = 2$. We recall that we use Cartesian space–time meshes with uniform partitions along each direction.

5.2.1 h -convergence

Singular time-independent potential ($V(x, y) = 1 - 1/x^2 - 1/y^2$) We consider the $(2 + 1)$ -dimensional problem on $Q_T = (0, 1)^2 \times (0, 1)$ with exact solution (see [33])

$$\psi(x, y, t) = x^2 y^2 e^{it}. \quad (5.6)$$

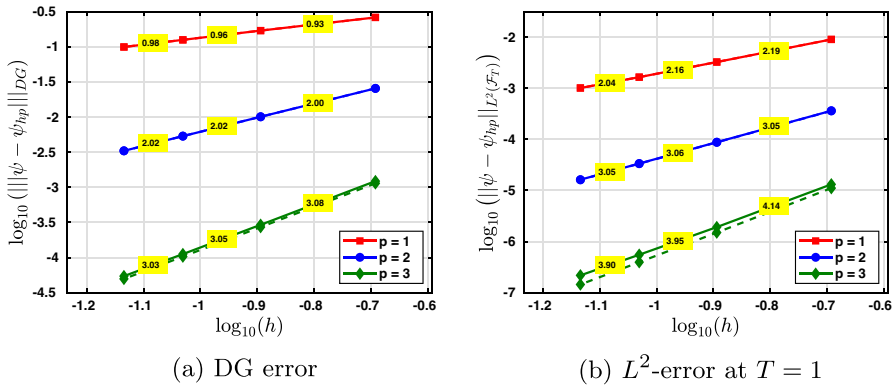


Fig. 11 h -convergence for the (2 + 1)-dimensional problem with potential $V(x, y) = 1 - 1/x^2 - 1/y^2$ and exact solution (5.6)

In Fig. 11, we show the errors obtained for a sequence of meshes with $h_x = h_y = h_t = 0.1, 0.0667, 0.05, 0.04$ and different degrees of approximation p . As in the numerical results for the (1 + 1)-dimensional problems, we obtain rates of convergence of order $\mathcal{O}(h^p)$ in the DG norm, and $\mathcal{O}(h^{p+1})$ in the L^2 norm at the final time.

Time-dependent potential ($V(x, y, t) = 2 \tanh^2(\sqrt{2}x) - 4(t - 1/2)^3 + 2 \tanh^2(\sqrt{2}y) - 2$) We now consider a manufactured problem with a time-dependent potential (see [7]). On the space–time domain $Q_T = (0, 1)^2 \times (0, 1)$ the exact solution is

$$\psi(x, y, t) = i e^{i(t-1/2)^4} \operatorname{sech}(x) \operatorname{sech}(y). \quad (5.7)$$

In Fig. 12 we show the errors obtained for the sequence of meshes from the previous experiment, and optimal convergence is observed in both norms.

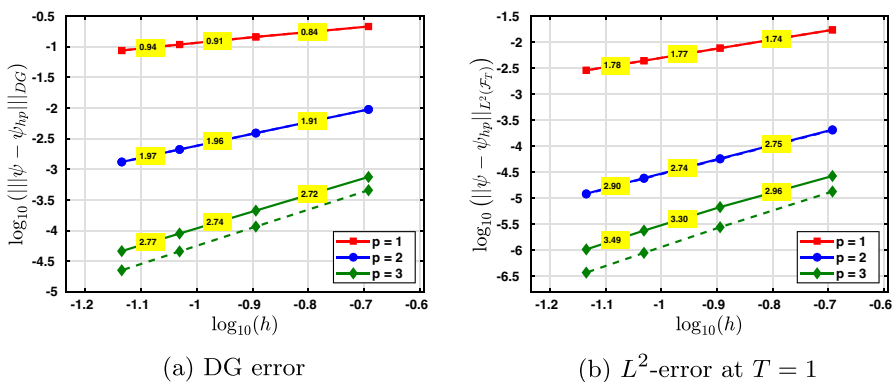


Fig. 12 h -convergence for the (2 + 1)-dimensional problem with time-dependent potential $V(x, y, t) = 2 \tanh^2(\sqrt{2}x) - 4(t - 1/2)^3 + 2 \tanh^2(\sqrt{2}y) - 2$ and exact solution (5.7)

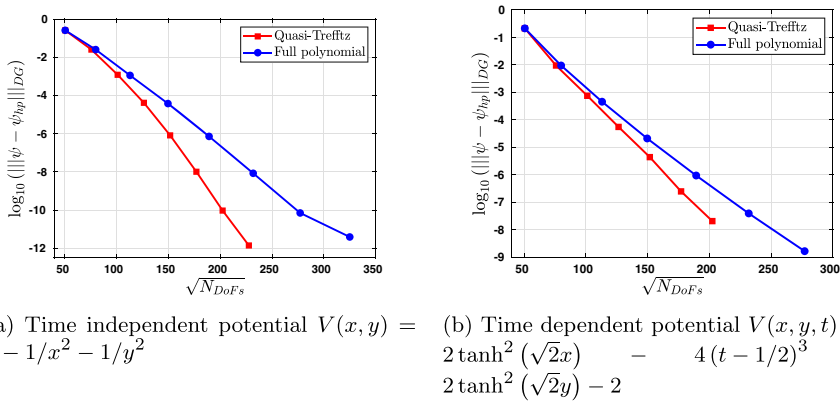


Fig. 13 p -convergence for the $(2 + 1)$ -dimensional problems

5.2.2 p -convergence

In Fig. 13 we show the results obtained for the p -version of the method applied to the $(2+1)$ -dimensional problems above, on the coarsest mesh. As expected, for the $(2+1)$ -dimensional case, the error of the quasi-Trefftz version decays root-exponentially as $\mathcal{O}(e^{-b\sqrt{N_{DoFs}}})$.

6 Concluding remarks

We have introduced a space–time ultra-weak discontinuous Galerkin discretization for the linear Schrödinger equation with variable potential. The DG method is well-posed and quasi-optimal in mesh-dependent norms for any space dimension $d \in \mathbb{N}$, and for very general prismatic meshes and discrete spaces. We proved optimal h -convergence of order $\mathcal{O}(h^p)$, in such a mesh-dependent norm, for two choices of the discrete spaces: the space of piecewise polynomials, and a novel quasi-Trefftz polynomial space with much smaller dimension. When the space–time mesh has a time-slab structure, the method allows for the decomposition of the resulting global linear system into a sequence of smaller problems on each time-slab: this is equivalent to an implicit time-stepping, possibly with local refinement in space–time. We present several numerical experiments that validate the accuracy of the method for different potentials and high-order approximations.

Acknowledgements We thank the anonymous reviewers for their valuable comments and suggestions.

Funding Open access funding provided by Università degli Studi di Milano - Bicocca within the CRUI-CARE Agreement. The authors received support from GNCS-INDAM, from PRIN projects “NA-FROM-PDEs” and “ASTICE”, and from PNRR-M4C2-I1.4-NC-HPC-Spoke6 funded by European Union – NextGenerationEU.

Declarations

Conflict of interest The authors declare no competing interests.

Open Access This article is licensed under a Creative Commons Attribution 4.0 International License, which permits use, sharing, adaptation, distribution and reproduction in any medium or format, as long as you give appropriate credit to the original author(s) and the source, provide a link to the Creative Commons licence, and indicate if changes were made. The images or other third party material in this article are included in the article's Creative Commons licence, unless indicated otherwise in a credit line to the material. If material is not included in the article's Creative Commons licence and your intended use is not permitted by statutory regulation or exceeds the permitted use, you will need to obtain permission directly from the copyright holder. To view a copy of this licence, visit <http://creativecommons.org/licenses/by/4.0/>.

References

1. Banjai, L., Georgoulis, E., Lijoka, O.: A Trefftz polynomial space-time discontinuous Galerkin method for the second order wave equation. *SIAM J. Num. Anal.* **55**(1), 63–86 (2017)
2. Born, M., Oppenheimer, R.: On the quantum theory of molecules. In *Quantum Chemistry: Classic Scientific Papers*, pp 1–24. World Scientific, (2000)
3. Brenner, S., Scott, R.: The mathematical theory of finite element methods, volume 15. Springer Science & Business Media, (2007)
4. Callahan, J.: Advanced calculus: a geometric view. Springer Science & Business Media, (2010)
5. Crandall, R., Litt, B.: Reassembly and time advance in reflectionless scattering. *Ann. Phys.* **146**(2), 458–469 (1983)
6. Dahl, J., Springborg, M.: The Morse oscillator in position space, momentum space, and phase space. *J. Chem. Phys.* **88**(7), 4535–4547 (1988)
7. Dehghan, M., Shokri, A.: A numerical method for two-dimensional Schrödinger equation using collocation and radial basis functions. *Comp. & Math. with Appl.* **54**(1), 136–146 (2007)
8. Demkowicz, L., Gopalakrishnan, J., Nagaraj, S., Sepulveda, P.: A spacetime DPG method for the Schrödinger equation. *SIAM J. Num. Anal.* **55**(4), 1740–1759 (2017)
9. Durán, R.: On polynomial approximation in Sobolev spaces. *SIAM J. Num. Anal.* **20**(5), 985–988 (1983)
10. Egger, H., Kretschmar, F., Schnepf, S., Weiland, T.: A space-time discontinuous Galerkin Trefftz method for time dependent Maxwell's equations. *SIAM J. Sci. Comput.* **37**(5), B689–B711 (2015)
11. Gómez, S., Moiola, A.: A space-time Trefftz discontinuous Galerkin method for the linear Schrödinger equation. *SIAM J. Num. Anal.* **60**(2), 688–714 (2022)
12. Gómez, S., Moiola, A., Perugia, I., Stocker, P.: On polynomial Trefftz spaces for the linear time-dependent Schrödinger equation. *Appl. Math. Lett.*, 146 (C): 108824, (2023)
13. Griffiths, D.: Introduction to Quantum Mechanics. Prentice-Hall, New York (1995)
14. Hain, S., Urban, K.: An ultra-weak space-time variational formulation for the Schrödinger equation. [arXiv:2212.14398](https://arxiv.org/abs/2212.14398), (2022)
15. Hiptmair, R., Moiola, A., Perugia, I.: Error analysis of Trefftz-discontinuous Galerkin methods for the time-harmonic Maxwell equations. *Math. Comp.* **82**(281), 247–268 (2013)
16. Hiptmair, R., Moiola, A., Perugia, I.: A survey of Trefftz methods for the Helmholtz equation. In *Building bridges: connections and challenges in modern approaches to numerical partial differential equations*, Springer, pp 237–279 (2016)
17. Imbert-Gérard, L.-M., Després, B.: A generalized plane-wave numerical method for smooth nonconstant coefficients. *IMA J. Num. Anal.* **34**(3), 1072–1103 (2014)
18. Imbert-Gérard, L.-M., Monk, P.: Numerical simulation of wave propagation in inhomogeneous media using generalized plane waves. *ESAIM Math. Model. Numer. Anal.* **51**(4), 1387–1406 (2017)
19. Imbert-Gérard, L.-M., Moiola, A., Stocker, P.: A space-time quasi-Trefftz DG method for the wave equation with piecewise-smooth coefficients. *Math. Comp.* **92**(341), 1211–1249 (2023)
20. Karakashian, O., Makridakis, C.: A space-time finite element method for the nonlinear Schrödinger equation: the discontinuous Galerkin method. *Math. Comp.* **67**(222), 479–499 (1998)

21. Karakashian, O., Makridakis, C.: A space-time finite element method for the nonlinear Schrödinger equation: the continuous Galerkin method. *SIAM J. Num. Anal.* **36**(6), 1779–1807 (1999)
22. Keller, J., Papadakis, J.: Wave propagation and underwater acoustics. Springer, (1977)
23. Lehrenfeld, C., Stocker, P.: Embedded Trefftz discontinuous Galerkin methods. *Int. J. Num. Methods Eng.* **124**(17), 3637–3661 (2023)
24. M. Levy. Parabolic equation methods for electromagnetic wave propagation. Number 45. IET, (2000)
25. Lifshitz, E., Landau, L.: Quantum Mechanics. Pergamon Press, Non-relativistic Theory (1965)
26. Lions, J.-L., Magenes, E.: Non-homogeneous boundary value problems and applications., vol. I. Die Grundlehren der mathematischen Wissenschaften, Band 181. Springer-Verlag, New York-Heidelberg, (1972)
27. Moiola, A., Perugia, I.: A space-time Trefftz discontinuous Galerkin method for the acoustic wave equation in first-order formulation. *Numer. Math.* **138**(2), 389–435 (2018)
28. Morse, P.: Diatomic molecules according to the wave mechanics. II. Vibrational levels. *Physical review* **34**(1), 57 (1929)
29. Olver, F., Lozier, D.W., Boisvert, R.F., Clark, C.: NIST handbook of mathematical functions. Cambridge university press, (2010)
30. Perugia, I., Schöberl, J., Stocker, P., Wintersteiger, C.: Tent pitching and Trefftz-DG method for the acoustic wave equation. *Comput. Math. Appl.* **79**(10), 2987–3000 (2020)
31. Qin, Q.-H.: Trefftz finite element method and its applications. *Appl. Mech. Rev.* **58**(5), 316–337 (2005)
32. Steinbach, O.: Space-time finite element methods for parabolic problems. *Comput. Methods Appl. Math.* **15**(4), 551–566 (2015)
33. Subaşı, M.: On the finite-differences schemes for the numerical solution of two dimensional Schrödinger equation. *Numer. Meth. for PDE: An International Journal*, 18 (6): 752–758, (2002)

Publisher's Note Springer Nature remains neutral with regard to jurisdictional claims in published maps and institutional affiliations.